J Sci Comput (2014) 59:688–720
DOI 10.1007/s10915-013-9778-9

A Local Discontinuous Galerkin Method for the Propagation of Phase Transition in Solids and Fluids

Lulu Tian · Yan Xu · J. G. M. Kuerten · J. J. W. Van der Vegt

Received: 19 March 2013 / Revised: 21 August 2013 / Accepted: 26 August 2013 /
Published online: 4 September 2013

Abstract A local discontinuous Galerkin (LDG) finite element method for the solution of a hyperbolic–elliptic system modeling the propagation of phase transition in solids and fluids is presented. Viscosity and capillarity terms are added to select the physically relevant solution. The L^2-stability of the LDG method is proven for basis functions of arbitrary polynomial order. In addition, using a priori error analysis, we provide an error estimate for the LDG discretization of the phase transition model when the stress–strain relation is linear, assuming that the solution is sufficiently smooth and the system is hyperbolic. Also, results of a linear stability analysis to determine the time step are presented. To obtain a reference exact solution we solved a Riemann problem for a trilinear strain–stress relation using a kinetic relation to select the unique admissible solution. This exact solution contains both shocks and phase transitions. The LDG method is demonstrated by computing several model

The research of L. Tian was supported by the China Scholarship Council (CSC). Research of J.J.W. van der Vegt was partially supported by the High-end Foreign Experts Recruitment Program (GDW20137100168), while the author was in residence at the University of Science and Technology of China.

Yan Xu received research supported from NSFC Grant Nos. 11371342, 11031007, FANEDD No. 200916, NCET No. 09-0922, Fok Ying Tung Education Foundation No. 131003.

L. Tian · J. J. W. Van der Vegt · J. G. M. Kuerten
Department of Applied Mathematics, University of Twente,
P.O. Box 217, 7500 AE Enschede, The Netherlands
e-mail: l.tian@utwente.nl

J. J. W. Van der Vegt
e-mail: j.j.w.vandervegt@utwente.nl

J. G. M. Kuerten
e-mail: J.G.M.Kuerten@tue.nl

Y. Xu (✉)
School of Mathematical Sciences, University of Science and Technology of China,
Hefei 230026 , Anhui, People's Republic of China
e-mail: yxu@ustc.edu.cn

problems representing phase transition in solids and in fluids with a Van der Waals equation of state. The results show the convergence properties of the LDG method.

Keywords Phase transition problem · Hyperbolic–elliptic system · Local discontinuous Galerkin · L^2-stability · A priori error analysis · Linear stability analysis

Mathematics Subject Classification (2000) 65M60 · 35Q79

1 Introduction

The propagation of phase transition in solids and fluids can be modeled with hyperbolic–elliptic systems of partial differential equations (PDEs). Examples are solid–solid transformations in elastic materials [2] and a homogeneous compressible fluid with liquid and vapor phases with a van der Waals equation of state [24]. A well-known one-dimensional hyperbolic–elliptic model that describes these phase transition phenomena is given by the following PDEs

$$\begin{cases} \gamma_t - v_x = 0, \\ v_t - (\sigma(\gamma))_x = 0, \end{cases} \tag{1.1}$$

where γ, v represent the deformation gradient (the strain) and velocity, respectively, and σ is the stress. We consider a stress–strain relation $\sigma(\gamma)$ as sketched in Fig. 1. The system (1.1) is hyperbolic for $\sigma'(\gamma) > 0$ and elliptic for $\sigma'(\gamma) < 0$. This mixed type hyperbolic–elliptic system contains a rich mathematical structure. For example, the standard entropy condition for a hyperbolic system is insufficient to determine the unique solution. This has stimulated an extensive analysis to investigate conditions that ensure the uniqueness of solutions of hyperbolic–elliptic systems, in particular their Riemann solutions. For an overview of the general theory, we refer to [19].

The need to impose additional conditions to ensure uniqueness of the solution originates from the fact that in the model equations small scale mechanisms that are induced by viscosity, capillarity and heat conduction are neglected [3]. One way to reintroduce the neglected physical information is the viscosity-capillarity (VC) approach. In the VC approach, solutions

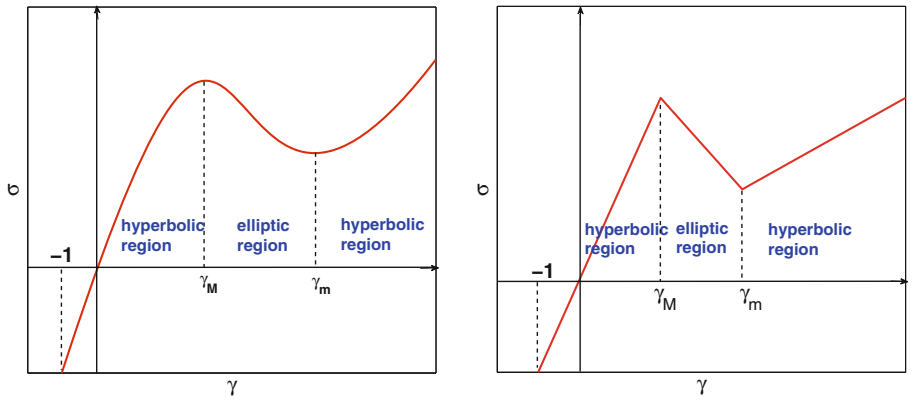

Fig. 1 Examples of strain–stress relation $\sigma(\gamma)$, general and trilinear case

of (1.1) are obtained by taking the limit of the solution of the system:

$$\begin{cases} \widetilde{\gamma}_t - \widetilde{v}_x = 0, \\ \widetilde{v}_t - (\sigma(\widetilde{\gamma}))_x = \nu \widetilde{v}_{xx} - \lambda \widetilde{\gamma}_{xxx}, \end{cases} \tag{1.2}$$

when the parameters ν and λ tend to zero, while the number $\omega = 2\sqrt{\lambda}/\nu$ is fixed. The notion of VC solutions for the equations describing a Van der Waals fluid was first proposed by Slemrod [23] based on Korteweg's theory of capillarity.

The solution of hyperbolic–elliptic systems may contain nonclassical shock waves or subsonic propagating phase transitions. Such waves do not satisfy standard entropy criteria and require an additional kinetic relation to select the unique admissible solution. For details of the theory of both classical and nonclassical shock waves, we refer to [19]. In particular, for the trilinear approximation to the stress–strain curve $\sigma(\gamma)$, Abeyaratne and Knowles [2] derived the exact solution of (1.1) containing both shock waves and phase boundaries. The kinetic relation and initiation criterion for the relevant phase transition must, however, be provided separately using physical modeling. Later, in [1], Abeyaratne and Knowles pointed out that a kinetic relation for (1.1) can also be obtained by considering traveling wave solutions for the augmented system (1.2) that includes viscosity and capillarity terms.

The numerical solution of mixed hyperbolic–elliptic systems, such as (1.1), is non-trivial. Standard numerical schemes smear out discontinuities and cause spurious solutions at the elliptic–hyperbolic boundary. Also, commonly used stabilization techniques, such as limiters, are counter productive for diffusive-dispersive regularization as given by the VC-equations (1.2).

One way to obtain accurate numerical discretizations for hyperbolic–elliptic systems is to use Glimm random choice methods [18] or front tracking techniques [4–6,10,11,20,29]. These methods use the exact solution of Riemann problems and resolve the phase boundary over one cell. They converge to the correct solutions of the non-classical Riemann problem. For complicated systems of hyperbolic–elliptic PDEs the use of an exact Riemann problem is, however, non-trivial, in particular in multiple dimensions.

An alternative is provided by finite difference and finite element discretizations of the VC-equations (1.2) using numerical methods that were originally developed to capture shocks and contact discontinuities in hyperbolic PDEs. Both for finite difference and finite element methods extensive research has been conducted to ensure that stable and high order accurate numerical solutions are obtained without spurious oscillations at phase boundaries, see e.g. [3,7,8,15,16]. This is non-trivial and still a topic of ongoing research.

In this article we will investigate the use of the local discontinuous Galerkin (LDG) finite element method for the solution of the VC-equations (1.2). The LDG method is an extension of the discontinuous Galerkin (DG) method that aims to solve PDEs that contain higher than first order spatial derivatives and was originally developed by Cockburn and Shu in [14] for solving nonlinear convection-diffusion equations containing second-order spatial derivatives. The idea behind LDG methods is to rewrite equations with higher order derivatives as a first order system, then apply the DG method to this extended system. The design of the numerical fluxes is the key ingredient for ensuring stability. LDG techniques have been developed for convection diffusion equations [14], nonlinear KdV type equations [28], the Camassa–Holm equation [25] and many other types of PDEs. For a review, see [26]. The LDG method results in an extremely local discretization, which offers great advantages in parallel computing and is well suited for *hp*-adaptation. In particular, the LDG method offers provable nonlinear stability. The LDG method for the VC-equations (1.2) that we describe in this paper shares all these elegant properties.

Recently, the LDG method was also used in [17] for the solution of the VC-equations (1.2) including a non-local convolution type regularization of (1.1). For this non-local model discretized with piecewise constant basis functions and central numerical fluxes in the LDG discretization, Haink and Rohde proved in Theorem 3.1 in [17] a discrete energy estimate. In this article we will prove a general L^2-stability estimate for the LDG discretization of (1.2) using alternating numerical fluxes and basis functions of arbitrary polynomial order. This L^2-stability estimate is also crucial for the a priori error analysis in which we prove that the LDG discretization is of optimal order. Another important topic we address is a detailed comparison of the LDG solutions with exact solutions of Riemann problems containing both phase transitions and shocks. For this purpose, we use the detailed analysis provided in [1,2].

The outline of the article is as follows. In Sect. 2 we present the LDG discretization for (1.2). Next, in Sect. 3 the L^2-stability of the LDG scheme is proven and an error estimate of the semi-discrete LDG scheme is given in Sect. 4. In Sect. 5, we discuss a linear stability analysis of the LDG method for the VC-equations. Numerical experiments for phase transition in solids and fluids, including the Van der Waals model [9], are described in Sect. 6. Special attention is given to demonstrate that solutions of the LDG method consistently converge to exact solutions of the phase transition model (1.1). Finally, conclusions are drawn in Sect. 7.

2 LDG Discretization Using the Viscosity–Capillarity Approach

2.1 Notation

We denote the mesh in the domain $\Omega \subset \mathbf{R}$ by $K_j = (x_{j-1/2}, x_{j+1/2})$, for $j = 1, \ldots, M$. The center of an element is $x_j = \frac{1}{2}(x_{j-1/2} + x_{j+1/2})$ and the mesh size is denoted by $h_j = x_{j+1/2} - x_{j-1/2}$, with $h = \max_{1\le j\le M} h_j$ being the maximum mesh size. We assume that the mesh is regular, namely the ratio between the maximum and the minimum mesh size stays bounded during mesh refinement. We define the space V_h^k as the space of polynomials of degree up to k in each element K_j, i.e.

$$V_h^k = \left\{ v \in L^2(\Omega) : v(x) \in P^k(K_j) \text{ for } x \in K_j,\ j = 1, \ldots M \right\}.$$

Note that functions in V_h^k are allowed to be discontinuous across element faces. For $P^k(K_j)$, we use Legendre polynomials as basis functions in V_h^k throughout this article.

The numerical solution is denoted by u_h, and belongs to the finite element space V_h^k. We denote by $(u_h)^-_{j+1/2}$ and $(u_h)^+_{j+1/2}$ the traces of u_h at $x_{j+1/2}$, taken from the left element K_j, and the right element K_{j+1}, respectively. We use the standard notation $[u_h] = u_h^+ - u_h^-$ to denote the jump of u_h at each element boundary point.

2.2 LDG Discretization

In this section, we present the LDG method for the VC-equations (1.2), which are defined as:

$$\begin{cases} \gamma_t = v_x, \\ v_t = (\sigma(\gamma))_x + \nu v_{xx} - \lambda \gamma_{xxx}, \end{cases} \tag{2.1}$$

with initial conditions:

$$\begin{cases} \gamma(x,0) = \gamma_0(x), \\ v(x,0) = v_0(x). \end{cases} \tag{2.2}$$

To define the LDG scheme, we first rewrite (2.1) as a first-order system:

$$\begin{cases} \gamma_t = v_x, \\ v_t = f_x + \nu q_x - \lambda s_x, \end{cases} \tag{2.3}$$

where we introduced the auxiliary variables f, s, p and q, which satisfy the equations:

$$\begin{cases} f = \sigma(\gamma), \\ s = p_x, \\ p = \gamma_x, \\ q = v_x. \end{cases} \tag{2.4}$$

The LDG method for (2.3), when f, q and s are assumed known, can be formulated as: find $\gamma_h, v_h \in V_h^k$, such that for all test functions $\phi,\ \varphi \in V_h^k$,

$$\begin{aligned} &\int_{K_j} (\gamma_h)_t \phi dx + \int_{K_j} v_h \phi_x dx - \widehat{v_h}\phi^-|_{j+1/2} + \widehat{v_h}\phi^+|_{j-1/2} = 0, \\ &\int_{K_j} (v_h)_t \varphi dx + \int_{K_j} f_h \varphi_x dx - \widehat{f_h}\varphi^-|_{j+1/2} + \widehat{f_h}\varphi^+|_{j-1/2} \\ &\quad -\lambda \int_{K_j} s_h \varphi_x dx + \lambda \widehat{s_h}\varphi^-|_{j+1/2} - \lambda \widehat{s_h}\varphi^+|_{j-1/2} + \nu \int_{K_j} q_h \varphi_x dx \\ &\quad -\nu \widehat{q_h}\varphi^-|_{j+1/2} + \nu \widehat{q_h}\varphi^+|_{j-1/2} = 0, \quad j = 1, \ldots, M. \end{aligned} \tag{2.5}$$

The "hat" terms in the cell boundary contributions in (2.5), resulting from integration by parts, are the so-called "numerical fluxes", which are single-valued functions defined at the element boundaries and should be designed to ensure stability. Here we take the alternating numerical fluxes:

$$\widehat{v_h} = v_h^+, \quad \widehat{f_h} = f_h^-, \quad \widehat{s_h} = s_h^-, \quad \widehat{q_h} = q_h^-. \tag{2.6}$$

Similarly, we derive for the auxiliary equations (2.4) the following LDG discretization: find $f_h, s_h, p_h, q_h \in V_h^k$, such that for all test functions $\zeta, \eta, \xi, \tau \in V_h^k$,

$$\int_{K_j} f_h \zeta dx - \int_{K_j} \sigma(\gamma_h)\zeta dx = 0, \tag{2.7a}$$

$$\int_{K_j} s_h \eta dx + \int_{K_j} p_h \eta_x dx - \widehat{p_h}\eta^-|_{j+1/2} + \widehat{p_h}\eta^+|_{j-1/2} = 0, \tag{2.7b}$$

$$\int_{K_j} p_h \xi dx + \int_{K_j} \gamma_h \xi_x dx - \widehat{\gamma_h}\xi^-|_{j+1/2} + \widehat{\gamma_h}\xi^+|_{j-1/2} = 0, \tag{2.7c}$$

$$\int_{K_j} q_h \tau dx + \int_{K_j} v_h \tau_x dx - \widehat{v_h}\tau^-|_{j+1/2} + \widehat{v_h}\tau^+|_{j-1/2} = 0. \tag{2.7d}$$

The numerical fluxes in (2.7) are chosen as:

$$\widehat{p_h} = p_h^+, \quad \widehat{\gamma_h} = \gamma_h^-, \quad \widehat{v_h} = v_h^+. \tag{2.8}$$

We remark that the choice of numerical fluxes in (2.6) and (2.8) is not unique. We can, for example, also choose the following numerical fluxes:

$$\widehat{v_h} = v_h^-, \quad \widehat{\gamma_h} = \gamma_h^+, \quad \widehat{s_h} = s_h^+, \quad \widehat{p_h} = p_h^-, \quad \widehat{q_h} = q_h^+, \quad \widehat{f_h} = f_h^+. \tag{2.9}$$

In Sect. 3 we will prove that both the numerical fluxes (2.6), (2.8) and (2.9) result in an LDG discretization which is L^2- stable.

2.3 Time Discretization

Suppose that the coefficients of the polynomial expansions of $\gamma_h(x,t)$ and $v_h(x,t)$ in each element are given by

$$(\gamma_0(t), \gamma_1(t), \ldots, \gamma_k(t),\ v_0(t), v_1(t), \ldots, v_k(t)) \equiv U(t).$$

The LDG discretization (2.5) for γ_h and v_h then can be written as the ODE system:

$$\begin{cases} U_t = F(U,t), \\ U(0) = U_0, \end{cases} \tag{2.10}$$

which we discretize in time by the third-order accurate explicit Runge–Kutta time stepping method [22], given as:

$$\begin{cases} V = U^n + \Delta t F(U^n, t^n), \\ W = \dfrac{3}{4}U^n + \dfrac{1}{4}V + \dfrac{1}{4}\Delta t F(V, t^n + \Delta t), \\ U^{n+1} = \dfrac{1}{3}U^n + \dfrac{2}{3}W + \dfrac{2}{3}\Delta t F(W, t^n + \dfrac{1}{2}\Delta t). \end{cases} \tag{2.11}$$

3 L^2-Stability of the LDG Scheme

The solution of the VC equations (2.1) preserves energy. In [13] Cockburn and Gau proved that the related discrete energy is also preserved for the finite difference discretization they proposed. In this section, we will prove that the LDG scheme (2.5)–(2.8) also preserves a discrete energy. This implies L^2-stability of the LDG discretization and it is an important and necessary property to obtain a stable and robust LDG scheme.

Theorem 1 (L^2-stability of the LDG scheme) *Assume* $\frac{\partial W(\gamma)}{\partial \gamma} = \sigma(\gamma)$, *and define the discrete energy* E_h *as*

$$E_h = \sum_{j=1}^{M} \left(\int_{K_j} W(\gamma_h) dx + \frac{1}{2} \int_{K_j} v_h^2 dx + \frac{\lambda}{2} \int_{K_j} p_h^2 dx \right).$$

Then the discrete energy E_h *computed from the LDG discretization of the VC equations given by* (2.5)–(2.8) *satisfies the relation*

$$\frac{d}{dt} E_h = -\nu \sum_{j=1}^{M} \int_{K_j} (q_h)^2 dx, \tag{3.1}$$

when periodic boundary conditions are applied at the domain boundary.

Proof We first take the time derivative of (2.7c),

$$\int_{K_j}(p_h)_t\xi dx+\int_{K_j}(\gamma_h)_t\xi_x dx-\widehat{(\gamma_h)_t}\xi^-|_{j+1/2}+\widehat{(\gamma_h)_t}\xi^+|_{j-1/2}=0. \tag{3.2}$$

After choosing in (2.5), (2.7) and (3.2) the following test functions,

$$\phi=f_h-\lambda s_h,\ \varphi=v_h,\ \zeta=-(\gamma_h)_t,\ \eta=\lambda(\gamma_h)_t,\ \xi=\lambda p_h,\ \tau=\nu q_h,$$

we get

$$\int_{K_j}(\gamma_h)_t(f_h-\lambda s_h)dx+\int_{K_j}v_h(f_h-\lambda s_h)_x dx-\widehat{v_h}(f_h-\lambda s_h)^-|_{j+1/2}$$
$$+\widehat{v_h}(f_h-\lambda s_h)^+|_{j-1/2}=0, \tag{3.3a}$$
$$\int_{K_j}(v_h)_t v_h dx+\int_{K_j}(f_h+\nu q_h-\lambda s_h)(v_h)_x dx$$
$$-(\widehat{f_h}+\nu\widehat{q_h}-\lambda\widehat{s_h})v_h^-|_{j+1/2}+(\widehat{f_h}+\nu\widehat{q_h}-\lambda\widehat{s_h})v_h^+|_{j-1/2}=0, \tag{3.3b}$$
$$-\int_{K_j}f_h(\gamma_h)_t dx+\int_{K_j}\sigma(\gamma_h)(\gamma_h)_t dx=0, \tag{3.3c}$$
$$\lambda\int_{K_j}s_h(\gamma_h)_t dx+\lambda\int_{K_j}p_h((\gamma_h)_t)_x dx-\lambda\widehat{p_h}(\gamma_h)_t^-|_{j+1/2}$$
$$+\lambda\widehat{p_h}(\gamma_h)_t^+|_{j-1/2}=0, \tag{3.3d}$$
$$\lambda\int_{K_j}(p_h)_t p_h dx+\lambda\int_{K_j}(\gamma_h)_t(p_h)_x dx-\lambda\widehat{(\gamma_h)_t}p_h^-|_{j+1/2}$$
$$+\lambda\widehat{(\gamma_h)_t}p_h^+|_{j-1/2}=0, \tag{3.3e}$$
$$\nu\int_{K_j}q_h^2 dx+\nu\int_{K_j}v_h(q_h)_x dx-\nu\widehat{v_h}q_h^-|_{j+1/2}+\nu\widehat{v_h}q_h^+|_{j-1/2}=0. \tag{3.3f}$$

Adding (3.3a)–(3.3f), and integrating the divergence terms, we obtain:

$$\int_{K_j}\left((\gamma_h)_t\sigma(\gamma_h)+(v_h)_t v_h+\lambda(p_h)_t p_h\right)dx$$
$$+\nu\int_{K_j}q_h^2 dx+F_{j+1/2}-F_{j-1/2}+\Theta_{j-1/2}=0. \tag{3.4}$$

The numerical entropy fluxes are given by:

$$\begin{aligned}F&=v_h^-f_h^--\lambda s_h^-v_h^-+\lambda p_h^-(\gamma_h)_t^-+\nu q_h^-v_h^--\widehat{v_h}f_h^-+\lambda\widehat{v_h}s_h^-\\&\quad-\widehat{f_h}v_h^--\nu\widehat{q_h}v_h^-+\lambda\widehat{s_h}v_h^--\lambda\widehat{p_h}(\gamma_h)_t^--\lambda\widehat{(\gamma_h)_t}p_h^--\nu\widehat{v_h}q_h^-\\&=\lambda v_h^+s_h^--\lambda p_h^+(\gamma_h)_t^--\nu v_h^+q_h^--f_h^-v_h^+,\end{aligned}$$

where we used the numerical fluxes (2.6) and (2.8). The Θ term is given by

$$\begin{aligned}\Theta = &-[v_h f_h] + \lambda[s_h v_h] - \lambda\left[p_h(\gamma_h)_t\right] - \nu\,[q_h v_h] + \widehat{v_h}[f_h] - \lambda\widehat{v_h}[s_h] \\ &+\widehat{f_h}[v_h] + \nu\widehat{q_h}[v_h] - \lambda\widehat{s_h}[v_h] + \lambda\widehat{p_h}[(\gamma_h)_t] + \lambda\widehat{\gamma_h}_t[p_h] + \nu\widehat{v_h}[q_h].\end{aligned}$$

Using the definition of the numerical fluxes (2.6) and (2.8) and after some algebraic manipulation, we obtain:

$$\Theta = 0.$$

After summation of (3.4) over all j and applying periodic boundary conditions, all entropy fluxes cancel and we obtain the following expression for the rate of change of the discrete energy:

$$\begin{aligned}\frac{d}{dt}E_h(t) &\equiv \sum_{j=1}^{M}\int_{K_j}(\sigma(\gamma_h)(\gamma_h)_t + (v_h)_t v_h + \lambda(p_h)_t p_h)\,dx \\ &= -\nu\sum_{j=1}^{M}\int_{K_j}(q_h)^2 dx,\end{aligned} \tag{3.5}$$

which proves (3.1). □

Remark 1 From the proof of Theorem 1, we can see that it holds for a general nonlinear σ function, which is not always an increasing function. From the definition of $W(\gamma)$, it follows that the summation of $\sum_j \int_{K_j} W(\gamma_h)$ is in general not negative, since $\sigma(\gamma)$ is an increasing-decreasing-increasing function, thus $W(\gamma)$ is a double well function, the same definition of $W(\gamma)$ can be found in [13].

4 Error Estimates

In this section we will prove an error estimate for the LDG discretization of the phase transition model (1.1) and also for the VC-equations (2.1) when ν, λ are finite and strictly positive. In the proof, the stress–strain relation is linear and we assume that the system is hyperbolic.

4.1 Projection Operator

In what follows, we will use two projections $\pi^{\pm}$ from the Sobolev space $H^1(\Omega)$ onto the finite element space V_h^k,

$$\pi^{\pm} : H^1(\Omega) \to V_h^k,$$

which are defined as follows. Given a function $\psi \in H^1(\Omega)$ and an arbitrary element $K_j \subset \Omega$, $j = 1, \ldots, M$, the restriction of $\pi^{\pm}\psi$ to K_j is defined as the elements of $P^k(K_j)$ that satisfy:

$$\int_{K_j}(\pi^{+}\psi - \psi)\omega dx = 0,\ \forall\omega \in P^{k-1}(K_j),\ \pi^{+}\psi(x^{+}_{j-1/2}) = \psi(x^{+}_{j-1/2}), \tag{4.1a}$$

$$\int_{K_j}(\pi^{-}\psi - \psi)\omega dx = 0,\ \forall\omega \in P^{k-1}(K_j),\ \pi^{-}\psi(x^{-}_{j+1/2}) = \psi(x^{-}_{j+1/2}). \tag{4.1b}$$

For the projections mentioned above, it is easy to see (c.f. [12]) that,

$$||\pi^{\pm}\psi - \psi||_{\Omega} \leq Ch^{k+1}, \tag{4.2}$$

with the positive constant C only depending on u and independent of h. We will denote the standard L^2-inner product as $(\cdot,\ \cdot)_{\Omega}$ and the L^2-norm as $||\cdot||_{\Omega}$.

4.2 Notations and Lemmas for the LDG Discretization

The error analysis can be greatly simplified by introducing the DG discretization operator $\mathcal{D}$,

$$\mathcal{D}(\eta, \phi; \widehat{\eta}) = \sum_j \mathcal{D}_{K_j}(\eta, \phi; \widehat{\eta}), \tag{4.3}$$

where $\mathcal{D}_{K_j}(\eta, \phi; \widehat{\eta})$ is defined in each element K_j as:

$$\mathcal{D}_{K_j}(\eta, \phi; \widehat{\eta}) = -(\eta, \phi_x)_{K_j} + (\widehat{\eta}\phi^-)_{j+1/2} - (\widehat{\eta}\phi^+)_{j-1/2}. \tag{4.4}$$

The following lemma from [27] gives very useful relations for the operator $\mathcal{D}$.

Lemma 1 *The DG discretization operator* (4.3) *with periodic boundary conditions satisfies the following relations: for all* $\phi \in V_h^k$,

$$\mathcal{D}(\eta, \phi; \eta^-) + \mathcal{D}(\phi, \eta; \phi^+) = 0, \tag{4.5a}$$
$$\mathcal{D}(\eta, \phi; \eta^+) + \mathcal{D}(\phi, \eta; \phi^-) = 0, \tag{4.5b}$$
$$\mathcal{D}(\eta - \pi^-\eta, \phi; (\eta - \pi^-\eta)^-) = 0, \tag{4.5c}$$
$$\mathcal{D}(\eta - \pi^+\eta, \phi; (\eta - \pi^+\eta)^+) = 0. \tag{4.5d}$$

For the error analysis of the LDG scheme given by (2.5)–(2.8), we define the following two bilinear forms:

$$\begin{aligned}
\mathcal{A}(\gamma, v, s, p, q; \phi, \varphi, \eta, \xi, \tau) &= \sum_j \mathcal{A}_{K_j}(\gamma, v, s, p, q; \phi, \varphi, \eta, \xi, \tau), \\
\mathcal{B}(\gamma, v, s, p, q; \phi, \varphi, \eta, \xi, \tau) &= \sum_j \mathcal{B}_{K_j}(\gamma, v, s, p, q; \phi, \varphi, \eta, \xi, \tau),
\end{aligned} \tag{4.6}$$

with

$$\begin{aligned}
&\mathcal{A}_{K_j}(\gamma, v, s, p, q; \phi, \varphi, \eta, \xi, \tau) = \\
&\quad (\gamma_t, \phi)_{K_j} + (v_t, \varphi)_{K_j} + (s, \eta)_{K_j} + (p_t, \xi)_{K_j} + (q, \tau)_{K_j}, \\
&\mathcal{B}_{K_j}(\gamma, v, s, p, q; \phi, \varphi, \eta, \xi, \tau) = \\
&\quad -\mathcal{D}_{K_j}(v, \phi; v^+) - \sigma'\mathcal{D}_{K_j}(\gamma, \varphi; \gamma^-) - \nu\mathcal{D}_{K_j}(q, \varphi; q^-) + \lambda\mathcal{D}_{K_j}(s, \varphi; s^-) \\
&\quad -\mathcal{D}_{K_j}(p, \eta; p^+) - \mathcal{D}_{K_j}(\gamma_t, \xi; \gamma^-) - \mathcal{D}_{K_j}(v, \tau; v^+).
\end{aligned} \tag{4.7}$$

The LDG scheme for the VC equations (2.1), given by (2.5), (2.7a), (2.7b), (2.7d) and (3.2) and numerical fluxes (2.6), (2.8) can now be expressed as: find $\gamma_h,\ v_h,\ s_h,\ p_h,\ q_h \in V_h^k$, such that for all test functions $\phi, \varphi, \eta, \xi, \tau \in V_h^k$, the following relation is satisfied.

$$\mathcal{A}(\gamma_h, v_h, s_h, p_h, q_h; \phi, \varphi, \eta, \xi, \tau) + \mathcal{B}(\gamma_h, v_h, s_h, p_h, q_h; \phi, \varphi, \eta, \xi, \tau) = 0, \tag{4.8}$$

where we use in this formulation the time derivative of (2.7c), given by (3.2).

We also define the following error contributions:

$$\begin{aligned} e_\gamma &= \gamma - \gamma_h = \gamma - \pi^- \gamma + \pi^- e_\gamma, \quad e_v = v - v_h = v - \pi^+ v + \pi^+ e_v, \\ e_s &= s - s_h = s - \pi^- s + \pi^- e_s, \quad e_p = p - p_h = p - \pi^+ p + \pi^+ e_p, \\ e_q &= q - q_h = q - \pi^- q + \pi^- e_q. \end{aligned} \tag{4.9}$$

4.3 Error Estimates of the Initial Conditions

We choose the initial conditions as

$$\gamma_h(x,0) = \pi^- \gamma(x,0),\ v_h(x,0) = \pi^+ v(x,0), \tag{4.10}$$

then (4.2) gives

$$\begin{aligned} ||v(\cdot,0) - v_h(\cdot,0)||_\Omega &\le Ch^{k+1}, \\ ||\gamma(\cdot,0) - \gamma_h(\cdot,0)||_\Omega &\le Ch^{k+1}, \end{aligned} \tag{4.11}$$

which means

$$||\pi^+ e_v(t=0)||_\Omega \le Ch^{k+1},\ ||\pi^- e_\gamma(t=0)||_\Omega \le Ch^{k+1}. \tag{4.12}$$

From (2.7c), we can easily get

$$\begin{aligned} &\int_{K_j} (p(x,0) - p_h(x,0))\,\xi dx + \int_{K_j} (\gamma(x,0) - \gamma_h(x,0))\,\xi_x \\ &\quad - (\widehat{\gamma}(x,0) - \widehat{\gamma}_h(x,0))\,\xi^-|_{j+1/2} + (\widehat{\gamma}(x,0) - \widehat{\gamma}_h(x,0))\,\xi^+|_{j-1/2} = 0 \end{aligned} \tag{4.13}$$

For the choice $\widehat{\gamma} = \gamma^-$ using (4.10), we have

$$\int_{K_j} (p(x,0) - p_h(x,0))\,\xi dx = 0. \tag{4.14}$$

Choosing $\xi = \pi^- e_p(x,0)$, we then easily get the relation

$$||\pi^- e_p(t=0)||_\Omega \le Ch^{k+1}. \tag{4.15}$$

4.4 A Priori Error Estimate of the LDG Discretization

In the next theorem, we provide an error estimate for the LDG discretization (2.5)–(2.8) of the phase transition model (1.1) using the VC-equations (2.1) with ν, λ going to zero. We consider a linear stress–strain relation and assume that the system is hyperbolic.

Theorem 2 *Assume a linear stress–strain relation in the phase transition model* (1.1) *and the related VC-equations* (2.1) *with* $\sigma(\gamma) = \gamma_0 + \sigma'\gamma$, *where the constant* σ' *satisfies* $\sigma' \ge C_\sigma^2 > 0$. *Assume that the exact solution satisfies* $\gamma(t) \in H^{k+2}(\Omega)$, $v(t) \in H^{k+1}(\Omega)$ *for* $t \in (t_0, T]$ *on a domain* $\Omega \subset \mathbf{R}$ *with periodic boundary conditions. Let* $\gamma_h, v_h \in V_h^k$, *the space of element wise discontinuous polynomials of degree up to k, be the numerical solution of the semi-discrete LDG scheme* (2.5)–(2.8) *and initial condition* (4.10). *If the parameters* $\nu, \lambda \downarrow 0$, *with the number* $\omega = 2\sqrt{\lambda}/\nu$ *constant and* $\lambda \sim h$, *then the following error estimate for the LDG solution of* (1.1) *holds:*

$$\sigma' ||e_\gamma||_\Omega^2 + 2||e_v||_\Omega^2 \le Ch^{2k+2}, \tag{4.16}$$

where C depends on the final time T, $||\gamma||_{L^\infty(0,T);H^{k+2}(\Omega)}$, $||v||_{L^\infty(0,T);H^{k+1}(\Omega)}$ and $||\gamma_t||_{L^\infty(0,T);H^{k+1}(\Omega)}$.

Proof We give proof for the error estimates in the following steps.

- *Energy equation for the error estimates*

After choosing the test functions in (4.8) as

$$\phi = \sigma'\pi^- e_\gamma - \lambda\pi^- e_s, \varphi = \pi^+ e_v, \eta = \lambda\pi^- e_{\gamma_t}, \xi = \lambda\pi^+ e_p, \tau = \nu\pi^- e_q,$$

using the consistency of the LDG scheme and summation over all elements K_j, we obtain the following relation for the error

$$\begin{aligned}
&\mathcal{A}(\gamma - \gamma_h, v - v_h, s - s_h, p - p_h, q - q_h; \sigma'\pi^- e_\gamma - \lambda\pi^- e_s, \pi^+ e_v,\\
&\quad \lambda\pi^- e_{\gamma_t}, \lambda\pi^+ e_p, \nu\pi^- e_q) +\\
&\mathcal{B}(\gamma - \gamma_h, v - v_h, s - s_h, p - p_h, q - q_h; \sigma'\pi^- e_\gamma - \lambda\pi^- e_s, \pi^+ e_v,\\
&\quad \lambda\pi^- e_{\gamma_t}, \lambda\pi^+ e_p, \nu\pi^- e_q) = 0.
\end{aligned} \tag{4.17}$$

If we introduce now the relations for the error given by (4.9), we can express (4.17) as

$$\begin{aligned}
&\mathcal{A}(\gamma - \pi^-\gamma, v - \pi^+ v, s - \pi^- s, p - \pi^+ p, q - \pi^- q; \sigma'\pi^- e_\gamma - \lambda\pi^- e_s,\\
&\quad \pi^+ e_v, \lambda\pi^- e_{\gamma_t}, \lambda\pi^+ e_p, \nu\pi^- e_q) +\\
&\mathcal{B}(\gamma - \pi^-\gamma, v - \pi^+ v, s - \pi^- s, p - \pi^+ p, q - \pi^- q; \sigma'\pi^- e_\gamma - \lambda\pi^- e_s,\\
&\quad \pi^+ e_v, \lambda\pi^- e_{\gamma_t}, \lambda\pi^+ e_p, \nu\pi^- e_q) +\\
&\mathcal{A}(\pi^- e_\gamma, \pi^+ e_v, \pi^- e_s, \pi^+ e_p, \pi^- e_q; \sigma'\pi^- e_\gamma - \lambda\pi^- e_s, \pi^+ e_v, \lambda\pi^- e_{\gamma_t},\\
&\quad \lambda\pi^+ e_p, \nu\pi^- e_q) +\\
&\mathcal{B}(\pi^- e_\gamma, \pi^+ e_v, \pi^- e_s, \pi^+ e_p, \pi^- e_q; \sigma'\pi^- e_\gamma - \lambda\pi^- e_s, \pi^+ e_v, \lambda\pi^- e_{\gamma_t},\\
&\quad \lambda\pi^+ e_p, \nu\pi^- e_q) = 0.
\end{aligned} \tag{4.18}$$

Next, if we use the expressions for $\mathcal{A}$ and $\mathcal{B}$ given by (4.7) and the properties of the operator $\mathcal{D}$ defined in Lemma 1, we obtain after a lengthy but straightforward computation that

$$\begin{aligned}
&\mathcal{A}(\pi^- e_\gamma, \pi^+ e_v, \pi^- e_s, \pi^+ e_p, \pi^- e_q; \sigma'\pi^- e_\gamma - \lambda\pi^- e_s, \pi^+ e_v, \lambda\pi^- e_{\gamma_t},\\
&\quad \lambda\pi^+ e_p, \nu\pi^- e_q) +\\
&\mathcal{B}(\pi^- e_\gamma, \pi^+ e_v, \pi^- e_s, \pi^+ e_p, \pi^- e_q; \sigma'\pi^- e_\gamma - \lambda\pi^- e_s, \pi^+ e_v, \lambda\pi^- e_{\gamma_t},\\
&\quad \lambda\pi^+ e_p, \nu\pi^- e_q) =\\
&\quad \frac{1}{2}\frac{d}{dt}(\sigma'||\pi^- e_\gamma||_\Omega^2 + ||\pi^+ e_v||_\Omega^2 + \lambda||\pi^+ e_p||_\Omega^2) + \nu||\pi^- e_q||_\Omega^2.
\end{aligned} \tag{4.19}$$

Also, using (4.5c), (4.5d) in Lemma 1 and the properties of the projection operators $\pi^\pm$ given by (4.1), we obtain the relation

$$\begin{aligned}
&\mathcal{B}(\gamma - \pi^-\gamma, v - \pi^+ v, s - \pi^- s, p - \pi^+ p, q - \pi^- q; \sigma'\pi^- e_\gamma - \lambda\pi^- e_s,\\
&\pi^+ e_v, \lambda\pi^- e_{\gamma_t}, \lambda\pi^+ e_p, \nu\pi^- e_q)\\
&\quad = -\lambda\mathcal{D}\left((\gamma - \pi^-\gamma)_t, \pi^+ e_p; (\gamma - \pi^-\gamma)_t^-\right) - \nu\mathcal{D}(q - \pi^- q, \pi^+ e_v; (q - \pi^- q)^-)\\
&\quad -\mathcal{D}(v - \pi^+ v, \sigma'\pi^- e_\gamma - \lambda\pi^- e_s; (v - \pi^+ v)^+) - \sigma'\mathcal{D}(\gamma - \pi^-\gamma, \pi^+ e_v; (\gamma - \pi^-\gamma)^-)\\
&\quad +\lambda\mathcal{D}(s - \pi^- s, \pi^+ e_v; (s - \pi^- s)^-) - \lambda\mathcal{D}(p - \pi^+ p, \pi^- e_{\gamma_t}; (p - \pi^+ p)^+)\\
&\quad -\nu\mathcal{D}((v - \pi^+ v), \pi^- e_q; (v - \pi^+ v)^+)\\
&\quad = 0.
\end{aligned} \tag{4.20}$$

If we introduce now relations (4.19)–(4.20) into (4.18), and use (4.7), the error equation (4.18) can be simplified as

$$\frac{1}{2}\frac{d}{dt}(\sigma'||\pi^- e_\gamma||^2_\Omega + ||\pi^+ e_v||^2_\Omega + \lambda||\pi^+ e_p||^2_\Omega) + \nu||\pi^- e_q||^2_\Omega + \mathcal{G} - \lambda((\gamma - \pi^-\gamma)_t, \pi^- e_s)_\Omega + \lambda((s - \pi^- s), \pi^- e_{\gamma_t})_\Omega = 0, \tag{4.21}$$

where we define the following contribution

$$\mathcal{G} = \sigma'\left((\gamma - \pi^-\gamma)_t, \pi^- e_\gamma\right)_\Omega + ((v - \pi^+ v)_t, \pi^+ v)_\Omega + \lambda((p - \pi^+ e_p)_t, \pi^+ e_p)_\Omega + \nu(q - \pi^- q, \pi^- e_q)_\Omega. \tag{4.22}$$

In the following, we will give estimates for $\mathcal{G}$, $\lambda((\gamma - \pi^-\gamma)_t, \pi^- e_s)_\Omega$ and $\lambda((s - \pi^- s), \pi^- e_{\gamma_t})_\Omega$ separately.

- *Error estimate for* $\mathcal{G}$.

Using Cauchy's inequality with ϵ and the interpolation estimate (4.2), we can estimate $\mathcal{G}$ as

$$\begin{aligned}\mathcal{G} &\le \frac{\sigma'}{4\epsilon_1^2}||\gamma_t - \pi^-\gamma_t||^2_\Omega + \sigma'\epsilon_1^2||\pi^- e_\gamma||^2_\Omega + \frac{1}{4\epsilon_2^2}||v_t - \pi^+ v_t||^2_\Omega + \epsilon_2^2||\pi^+ e_v||^2_\Omega \\ &+ \frac{\lambda}{4\epsilon_3^2}||p_t - \pi^+ p_t||^2_\Omega + \lambda\epsilon_3^2||\pi^+ e_p||^2_\Omega + \frac{\nu}{4\epsilon_4^2}||q - \pi^- q||^2_\Omega + \nu\epsilon_4^2||\pi^- e_q||^2_\Omega \\ &\le Ch^{2k+2} + \sigma'\epsilon_1^2||\pi^- e_\gamma||^2_\Omega + \epsilon_2^2||\pi^+ e_v||^2_\Omega + \lambda\epsilon_3^2||\pi^+ e_p||^2_\Omega + \nu\epsilon_4^2||\pi^- e_q||^2_\Omega.\end{aligned} \tag{4.23}$$

with $\epsilon_i > 0$, $(i = 1, 2, 3, 4)$. Introducing (4.23) into (4.21) gives:

$$\begin{aligned}&\frac{1}{2}\frac{d}{dt}\left(\sigma'||\pi^- e_\gamma||^2_\Omega + ||\pi^+ e_v||^2_\Omega + \lambda||\pi^+ e_p||^2_\Omega\right) + \nu||\pi^- e_q||^2_\Omega \\ &-\lambda((\gamma - \pi^-\gamma)_t, \pi^- e_s)_\Omega + \lambda(s - \pi^- s, \pi^- e_{\gamma_t})_\Omega \le Ch^{2k+2} \\ &+\sigma'\epsilon_1^2||\pi^- e_\gamma||^2_\Omega + \epsilon_2^2||\pi^+ e_v||^2_\Omega + \lambda\epsilon_3^2||\pi^+ e_p||^2_\Omega + \nu\epsilon_4^2||\pi^- e_q||^2_\Omega.\end{aligned} \tag{4.24}$$

- *Error estimate for* $\lambda((\gamma - \pi^-\gamma)_t, \pi^- e_s)_\Omega$.

Next, we consider the contribution $\lambda((\gamma - \pi^-\gamma)_t, \pi^- e_s)_\Omega$. Using the Cauchy and Schwarz inequalities we obtain:

$$\lambda\left((\gamma - \pi^-\gamma)_t, \pi^- e_s\right)_\Omega \le \frac{1}{2}||\gamma_t - \pi^-\gamma_t||^2_\Omega + \frac{\lambda^2}{2}||\pi^- e_s||^2_\Omega. \tag{4.25}$$

The upper bound in (4.25) contains, however, $||\pi^- e_s||_\Omega$, which can not be directly bounded in (4.21). We therefore use the LDG equation (3.3d) together with the numerical fluxes (2.8) to derive the following error equation

$$(s - s_h, \eta)_{K_j} + (p - p_h, \eta_x)_{K_j} - \left((p - p_h)^+\eta^-\right)_{j+1/2} + \left((p - p_h)^+\eta^+\right)_{j-1/2} = 0, \quad \forall \eta \in V_h^k. \tag{4.26}$$

Using the error relations (4.9), we can transform (4.26) into

$$(s - \pi^- s, \eta)_{K_j} + (\pi^- e_s, \eta)_{K_j} + (\pi^+ e_p, \eta_x)_{K_j} - (\pi^+ e_p)^+\eta^-|_{j+1/2} + (\pi^+ e_p)^+\eta^+|_{j-1/2} = 0, \quad \forall \eta \in V_h^k. \tag{4.27}$$

Here, we used that

$$(p-\pi^+p,\eta_x)_{K_j}-(p-\pi^+p)^+\eta^-|_{j+1/2}+(p-\pi^+p)^+\eta^+|_{j-1/2}=0,$$

for the projection operator π^+ defined in (4.1) and $\eta\in V_h^k$.

The error equation (4.27) can be further evaluated using the following trace and inverse inequalities

$$|\eta(x_{j\pm\frac{1}{2}})|\le\frac{C_{trace}}{\sqrt{h}}||\eta||_{K_j},\quad ||\eta_x||_{K_j}\le\frac{C_{inv}}{h}||\eta||_{K_j},\quad \text{for}\,\eta\in V_h^k$$

and selecting $\eta=\pi^-e_s$. This provides an estimate for $||\pi^-e_s||_\Omega$ by summing over the elements K_j and introducing ϵ_5

$$||\pi^-e_s||_\Omega\le\frac{1}{2\sqrt{\epsilon_5}}||s-\pi^-s||_\Omega+\frac{\sqrt{\epsilon_5}}{2h}\left(C_{inv}+C_{trace}\right)||\pi^+e_p||_\Omega. \tag{4.28}$$

Collecting all contributions and using the interpolation estimate (4.2) then results in the following estimate for (4.25)

$$\begin{aligned}\lambda(\gamma_t-\pi^-\gamma_t,\pi^-e_s)_\Omega&\le\frac{1}{2}||\gamma_t-\pi^-\gamma_t||_\Omega^2+\frac{\lambda^2}{4\epsilon_5}||s-\pi^-s||_\Omega^2\\&+\frac{\epsilon_5}{4h^2}\lambda^2(C_{inv}+C_{trace})^2||\pi^+e_p||_\Omega^2.\end{aligned} \tag{4.29}$$

Note that the parameter λ in the VC system (2.1) goes to zero, so if we choose

$$\lambda\sim O(h),\quad \lambda=2C_1h, \tag{4.30}$$

(4.29) becomes

$$\lambda(\gamma_t-\pi^-\gamma_t,\pi^-e_s)_\Omega\le Ch^{2k+2}+\epsilon_5C_1^2\left(C_{inv}+C_{trace}\right)^2||\pi^+e_p||_\Omega^2. \tag{4.31}$$

Introducing (4.31) into (4.24) and after integration in time, we obtain,

$$\begin{aligned}&\frac{1}{2}\left(\sigma'||\pi^-e_\gamma||_\Omega^2+||\pi^+e_v||_\Omega^2+\lambda||\pi^+e_p||_\Omega^2\right)+\nu\int_0^t||\pi^-e_q||_\Omega^2dt\\&+\lambda\int_0^t(s-\pi^-s,\pi^-e_{\gamma_t})_\Omega dt\\&\le Ch^{2k+2}+\frac{1}{2}\sigma'||\pi^-e_\gamma(t=0)||_\Omega^2+\frac{1}{2}||\pi^+e_v(t=0)||_\Omega^2\\&+\frac{1}{2}\lambda||\pi^+e_p(t=0)||_\Omega^2+\int_0^t(\sigma'\epsilon_1^2||\pi^-e_\gamma||_\Omega^2+\epsilon_2^2||\pi^+e_v||_\Omega^2\\&+\nu\epsilon_4^2||\pi^-e_q||_\Omega^2+(\lambda\epsilon_3^2+\epsilon_5C_1^2(C_{inv}+C_{trace})^2)||\pi^+e_p||_\Omega^2)dt.\end{aligned} \tag{4.32}$$

Finally, introducing the estimates of the initial conditions (4.12) and (4.15) into (4.32) results in the estimate

$$\begin{aligned}
&\frac{1}{2}\left(\sigma'||\pi^- e_\gamma||_\Omega^2 + ||\pi^+ e_v||_\Omega^2 + \lambda||\pi^+ e_p||_\Omega^2\right) + \nu\int_0^t ||\pi^- e_q||_\Omega^2 dt \\
&\quad +\lambda\int_0^t (s-\pi^- s, \pi^- e_{\gamma_t})_\Omega dt \\
&\quad \le Ch^{2k+2} + \int_0^t (\sigma'\epsilon_1^2||\pi^- e_\gamma||_\Omega^2 + \epsilon_2^2||\pi^+ e_v||_\Omega^2 + \nu\epsilon_4^2||\pi^- e_q||_\Omega^2 \\
&\quad +(\lambda\epsilon_3^2 + \epsilon_5 C_1^2(C_{inv}+C_{trace})^2)||\pi^+ e_p||_\Omega^2)dt. \qquad (4.33)
\end{aligned}$$

- *Error estimate for* $\lambda\int_0^t (s-\pi^- s, \pi^- e_{\gamma_t})_\Omega dt$.

Consider now $\lambda\int_0^t (s-\pi^- s, \pi^- e_{\gamma_t})_\Omega dt$. Using (4.12), this contribution can be estimated straightforwardly as

$$\begin{aligned}
&\lambda\int_0^t \left(s-\pi^- s, \pi^- e_{\gamma_t}\right)_\Omega dt \\
&= \lambda\left(s-\pi^- s, \pi^- e_\gamma\right)|_0^t - \lambda\int_0^t (s_t-\pi^- s_t, \pi^- e_\gamma)dt \\
&\le \lambda||s-\pi^- s||_\Omega||\pi^- e_\gamma||_\Omega + \lambda||(s-\pi^- s)(t=0)||_\Omega||\pi^- e_\gamma(t=0)||_\Omega \\
&\quad +\lambda\int_0^t ||s_t-\pi^- s_t||_\Omega||\pi^- e_\gamma||_\Omega dt \\
&\le \frac{\lambda}{4\epsilon_6^2}||s-\pi^- s||_\Omega^2 + \lambda\epsilon_6^2||\pi^- e_\gamma||_\Omega^2 + \frac{\lambda}{4\epsilon_7^2}||(s-\pi^- s)(t=0)||_\Omega^2 \\
&\quad +\lambda\epsilon_7^2||\pi^- e_\gamma(t=0)||_\Omega^2 + \frac{\lambda}{4\epsilon_8^2}\int_0^t ||(s_t-\pi^- s_t)||_\Omega^2 dt + \lambda\epsilon_8^2\int_0^t ||\pi^- e_\gamma||_\Omega^2 dt \\
&\le Ch^{2k+2} + \lambda\epsilon_6^2||\pi^- e_\gamma||_\Omega^2 + \lambda\epsilon_8^2\int_0^t ||\pi^- e_\gamma||_\Omega^2 dt. \qquad (4.34)
\end{aligned}$$

Introducing (4.34) into (4.33) gives

$$\begin{aligned}
&\frac{1}{2}\left(\sigma'||\pi^- e_\gamma||_\Omega^2 + ||\pi^+ e_v||_\Omega^2 + \lambda||\pi^+ e_p||_\Omega^2\right) + \nu\int_0^t ||\pi^- e_q||_\Omega^2 dt \qquad (4.35) \\
&\le Ch^{2k+2} + \int_0^t (\sigma'\epsilon_1^2||\pi^- e_\gamma||_\Omega^2 + \epsilon_2^2||\pi^+ e_v||_\Omega^2 + \nu\epsilon_4^2||\pi^- e_q||_\Omega^2 \\
&+(\lambda\epsilon_3^2 + \epsilon_5 C_1^2(C_{inv}+C_{trace})^2)||\pi^+ e_p||_\Omega^2 + \lambda\epsilon_8^2||\pi^- e_\gamma||_\Omega^2)dt + \lambda\epsilon_6^2||\pi^- e_\gamma||_\Omega^2,
\end{aligned}$$

which is equivalent to

$$\left(\frac{1}{2}\sigma' - \lambda\epsilon_6^2\right)||\pi^- e_\gamma||_\Omega^2 + \frac{1}{2}||\pi^+ e_v||_\Omega^2 + \frac{\lambda}{2}||\pi^+ e_p||_\Omega^2 + \nu(1-\epsilon_4^2)\int_0^t ||\pi^- e_q||_\Omega^2 dt$$

$$\leq Ch^{2k+2} + \int_0^t \left(\left(\sigma'\epsilon_1^2 + \lambda\epsilon_8^2\right)||\pi^- e_\gamma||_\Omega^2 + \epsilon_2^2||\pi^+ e_v||_\Omega^2\right. \tag{4.36}$$

$$\left. + \left(\lambda\epsilon_3^2 + \epsilon_5 C_1^2 (C_{inv} + C_{trace})^2\right)||\pi^+ e_p||_\Omega^2\right) dt.$$

Choose now $\epsilon_1 = \frac{1}{2\sqrt{2}}$ and ϵ_6, ϵ_8 as

$$\epsilon_6 = \frac{1}{2}\sqrt{\frac{\sigma'}{\lambda}}, \text{ then } \frac{1}{2}\sigma' - \lambda\epsilon_6^2 = \frac{1}{4}\sigma',$$

$$\epsilon_8 = \frac{1}{2}\sqrt{\frac{\sigma'}{2\lambda}}, \text{ then } \sigma'\epsilon_1^2 + \lambda\epsilon_8^2 = \frac{1}{4}\sigma'. \tag{4.37}$$

Select $\epsilon_3 = \frac{1}{2}$ and ϵ_5 such that

$$\lambda\epsilon_3^2 + \epsilon_5 C_1^2 (C_{inv} + C_{trace})^2 = \frac{\lambda}{2}.$$

Finally, choosing $\epsilon_2 = \epsilon_4 = \frac{1}{\sqrt{2}}$, we obtain the inequality

$$\frac{\sigma'}{4}||\pi^- e_\gamma||_\Omega^2 + \frac{1}{2}||\pi^+ e_v||_\Omega^2 + \frac{\lambda}{2}||\pi^+ e_p||_\Omega^2$$

$$\leq Ch^{2k+2} + \int_0^t \left(\frac{\sigma'}{4}||\pi^- e_\gamma||_\Omega^2 + \frac{1}{2}||\pi^+ e_v||_\Omega^2 + \frac{\lambda}{2}||\pi^+ e_p||_\Omega^2\right) dt. \tag{4.38}$$

Since $\lambda \downarrow 0$, the final estimate for the error contributions is now obtained using Gronwall's Lemma for integrals, resulting in:

$$\max_t \frac{\sigma'}{4}||\pi^- e_\gamma||_\Omega^2 + \max_t \frac{1}{2}||\pi^+ e_v||_\Omega^2 \leq Ch^{2k+2}, \tag{4.39}$$

and using (4.9), (4.39) gives the result stated in Theorem 2. □

Remark 2 For the case $\lambda, \nu \downarrow 0$ with $\omega = 2\sqrt{\lambda}/\nu$ constant we obtain by choosing $\lambda = 2C_1 h$, ϵ_6, ϵ_8 as (4.37) and $0 < \epsilon_4 < 1$, that the bounding constant C in (4.16) is independent of ν and λ.

Corollary 1 *Under the assumptions of Theorem 2 except, that $\lambda, \nu > 0$ have finite, strictly positive values, the following error estimate holds,*

$$\sigma'||e_\gamma||_\Omega^2 + 2||e_v||_\Omega^2 + 2\lambda||e_p||_\Omega^2 \leq Ch^{2k},$$

where C depends on the final time T, $||\gamma||_{L^\infty(0,T);H^{k+2}(\Omega)}$, $||v||_{L^\infty(0,T);H^{k+1}(\Omega)}$ and $||\gamma_t||_{L^\infty(0,T);H^{k+1}(\Omega)}$.

Proof Since $\lambda > 0$ has a finite value, the term $\lambda(\gamma_t - \pi^-\gamma_t, \pi^- e_s)_\Omega$ in (4.29) should be estimated in a different way.

- *Error estimate for* $\lambda((\gamma - \pi^-\gamma)_t, \pi^- e_s)_\Omega$.

Using the Cauchy and Schwarz inequalities we obtain:

$$\lambda\left((\gamma-\pi^{-}\gamma)_t,\pi^{-}e_s\right)_{\Omega}\leq\frac{1}{2h^2}||\gamma_t-\pi^{-}\gamma_t||^2_{\Omega}+\frac{\lambda^2h^2}{2}||\pi^{-}e_s||^2_{\Omega}. \tag{4.40}$$

Using (4.28), (4.40) becomes

$$\lambda\left((\gamma-\pi^{-}\gamma)_t,\pi^{-}e_s\right)_{\Omega}\leq Ch^{2k}+\epsilon_5\frac{\lambda^2}{4}(C_{inv}+C_{trace})^2||\pi^{+}e_p||^2_{\Omega}. \tag{4.41}$$

The rest proof is similar to the proof of Theorem 2, finally we obtain the result stated in Corollary 1. □

5 Linear Stability Analysis of the LDG Scheme

In order to obtain a reasonable estimate for a stable time step for the third order accurate TVD Runge–Kutta scheme (2.11) applied to the LDG discretization, we perform in this section a linear stability analysis.

First, we explain the specific problem that we analyze. The parameters ν, λ in the VC-equations (2.1) are defined as in [13]:

$$\nu=2\nu_0,\quad \lambda=\omega^2\nu_0^2, \tag{5.1}$$

where

$$\nu_0=\left(\sup_{\gamma\geq-1}\max\{0,\sigma'(\gamma)\}\right)^{1/2}(\Delta x)^{\beta}, \tag{5.2}$$

for $\beta\in(0,1]$ and $\omega=2\sqrt{\lambda}/\nu$ a fixed number. We assume that the stress–strain relation $\sigma(\gamma)$ in (2.1) is a trilinear function, defined as

$$\sigma(\gamma)=\begin{cases}\mu_1\gamma, & \gamma\in(-1,\gamma_M),\\ -\mu_2\gamma+b, & \gamma\in(\gamma_M,\gamma_m),\\ \mu_3\gamma, & \gamma\in(\gamma_m,\infty),\end{cases} \tag{5.3}$$

see also Fig. 1. We thus consider locally a linear stress–strain relation $\sigma(\gamma)=\sigma'\gamma$, and assume that $\sigma'>0$. In the elliptic part, where $\sigma'<0$, the exact solution is unstable and γ will rapidly move to the hyperbolic part. The third order TVD Runge–Kutta time stepping method (2.11) has an amplification matrix Q, that is equal to

$$Q=Id+A+\frac{1}{2}A^2+\frac{1}{6}A^3, \tag{5.4}$$

with $A=\Delta t\,B$ and $F(U(t))=BU(t)$ after linearization of $\sigma(\gamma)$. For stability, the following condition on the operator norm of Q must hold

$$||Q||\leq 1, \tag{5.5}$$

which is equivalent in the hyperbolic part to

$$\left|1+\lambda_i+\frac{1}{2}\lambda_i^2+\frac{1}{6}\lambda_i^3\right|\leq 1, \tag{5.6}$$

with λ_i the eigenvalues of A for $i=1,\ldots,n$, and provides a restriction on the time step Δt. Since A depends on the polynomial order used in the LDG discretization, we will compute now the time step restriction for various polynomial orders.

Since the LDG matrix A has a block Toeplitz structure on a uniform mesh when periodic boundary conditions are applied, we can compute the eigenvalues using a discrete Fourier transform. For piecewise constant polynomials, we obtain the matrix

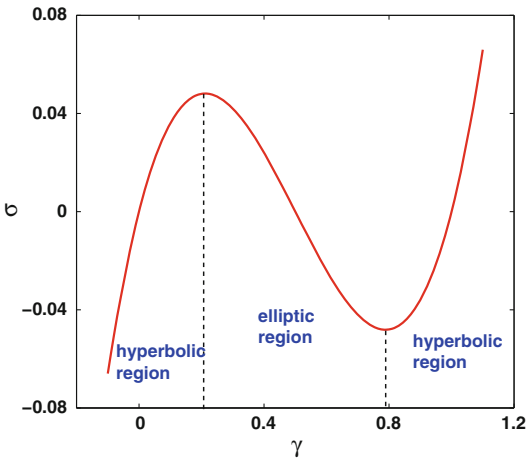

Fig. 2 Piecewise cubic strain–stress relation

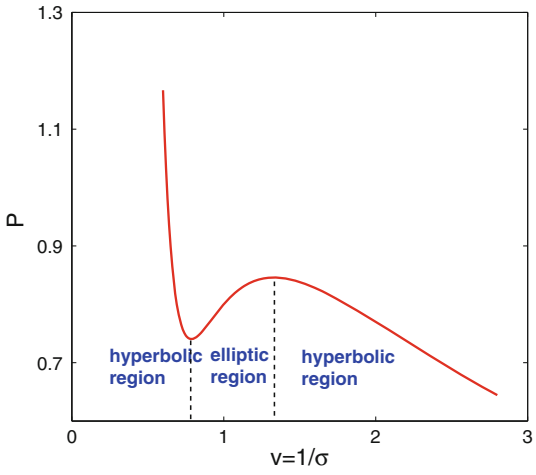

Fig. 3 Example of Van der Waals pressure law

$$\widehat{\mathbf{A}}(\theta) = \frac{\Delta t}{\Delta x}\begin{pmatrix} 0 & a \\ \sigma' b - \frac{\lambda}{\Delta x^2} ab^2 & \frac{\nu}{\Delta x} ab \end{pmatrix}, \tag{5.7}$$

with

$$a = e^{i\theta} - 1,\ b = 1 - e^{-i\theta},\ c = ab = -4\sin^2\left(\frac{\theta}{2}\right) \text{ and } \theta \in [-\pi, \pi).$$

The eigenvalues of $\widehat{\mathbf{A}}$, taking (5.1) and (5.2) into account, are equal to

$$\begin{aligned} \lambda_{1,2} &= \frac{\Delta t}{\Delta x}\frac{\nu}{\Delta x}\left(\frac{c}{2} \pm \sqrt{(1-\omega^2)\frac{c^2}{4} + \frac{\sigma' c}{(\nu/\Delta x)^2}}\right) \\ &= \Delta t \mu\left(c \pm \sqrt{(1-\omega^2)c^2 + \frac{\sigma' c}{\mu}}\right), \end{aligned} \tag{5.8}$$

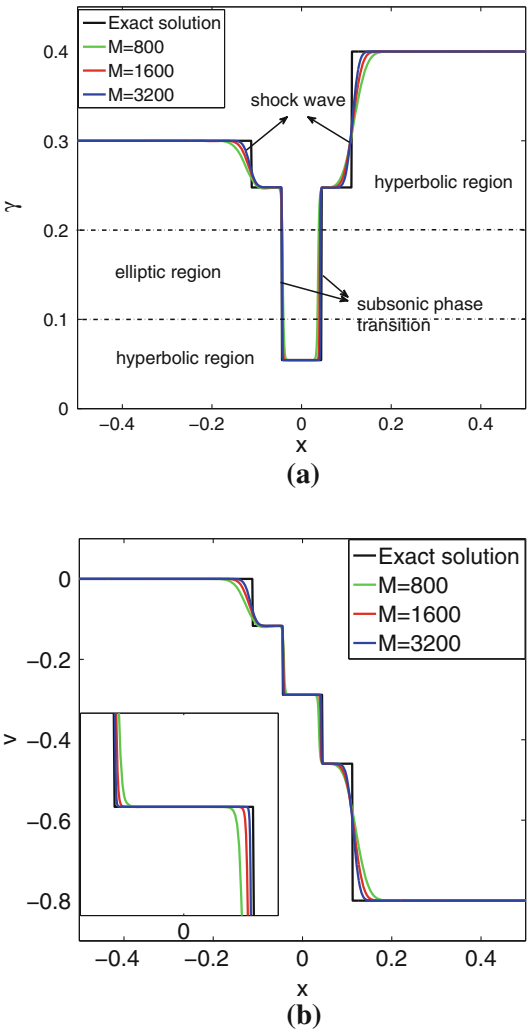

Fig. 4 Phase transitions and shocks in an elastic solid model with trilinear stress–strain relation σ, $\omega = 1.0$, initial condition A. **a** Strain γ. **b** Velocity v

with $\mu = \frac{\nu}{2(\Delta x)^2}$. Given a value of ω, σ' and μ we can compute now the time step Δt such that $\lambda_{1,2}$ satisfy (5.6) for all $\theta \in [-\pi, \pi)$.

For linear basis functions, we obtain the matrix $\widehat{\mathbf{A}}(\theta)$

$$\widehat{\mathbf{A}}(\theta) = \Delta t \begin{pmatrix} \mathbf{0} & p \\ \sigma' q - \lambda qpq & \nu qp \end{pmatrix} \begin{pmatrix} \gamma_0 \\ \gamma_1 \\ v_0 \\ v_1 \end{pmatrix}, \tag{5.9}$$

with

$$p = \frac{1}{\Delta x} \begin{pmatrix} e^{i\theta} - 1 & 1 - e^{i\theta} \\ 3(e^{i\theta} - 1) & -3(e^{i\theta} + 1) \end{pmatrix}, \; q = \frac{1}{\Delta x} \begin{pmatrix} 1 - e^{-i\theta} & 1 - e^{-i\theta} \\ 3(e^{-i\theta} - 1) & 3(1 + e^{-i\theta}) \end{pmatrix}.$$

The matrix $\widehat{\mathbf{A}}(\theta)$ has eigenvalues $\lambda_i(\theta)$, $i = 1, \ldots, 4$, which can be used to compute the time step constraint using (5.6) in the same way as done for constant basis functions. Unfortu-

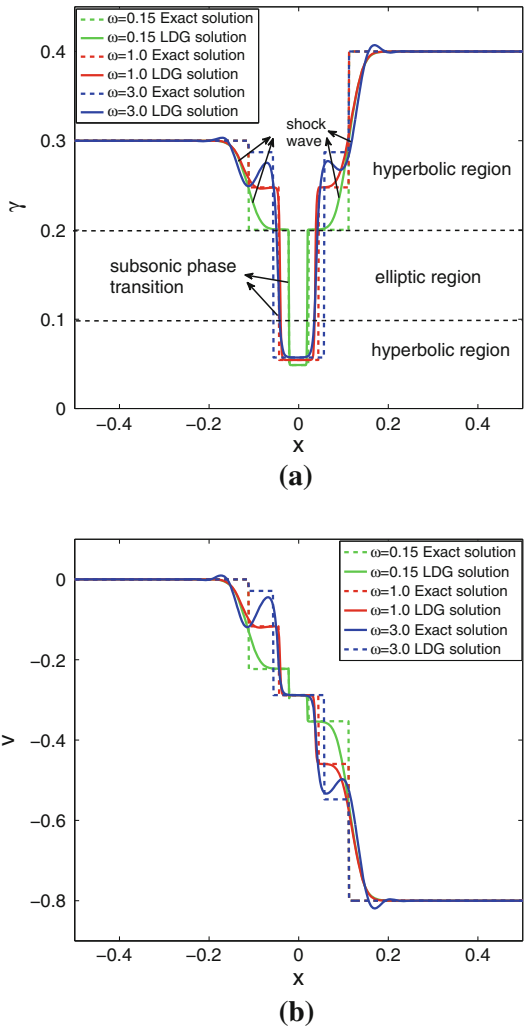

Fig. 5 Phase transitions and shocks in an elastic solid model with trilinear stress–strain relation σ, initial condition A, various ω, $M = 800$. **a** Strain γ. **b** Velocity v

nately, it is not possible to obtain completely analytic expressions for the time step. In the computations performed in the next section, we use the parameters $\max_\gamma \sigma' = 20$, $\beta = 1$ in (5.1), (5.2) and determine the time step $\Delta t = CFL\Delta x$ with

$$CFL \leq \begin{cases} 0.03, & \omega = 0.15, \\ 0.05, & \omega = 1.0, \\ 0.02, & \omega = 3.0, \end{cases} \tag{5.10}$$

for constant basis functions, and

$$CFL \leq \begin{cases} 0.006, & \omega = 0.15, \\ 0.008, & \omega = 1.0, \\ 0.01, & \omega = 3.0, \end{cases} \tag{5.11}$$

for linear basis functions. For quadratic basis functions, the numerical experiments show that the CFL bounds should be (5.11) divided by five.

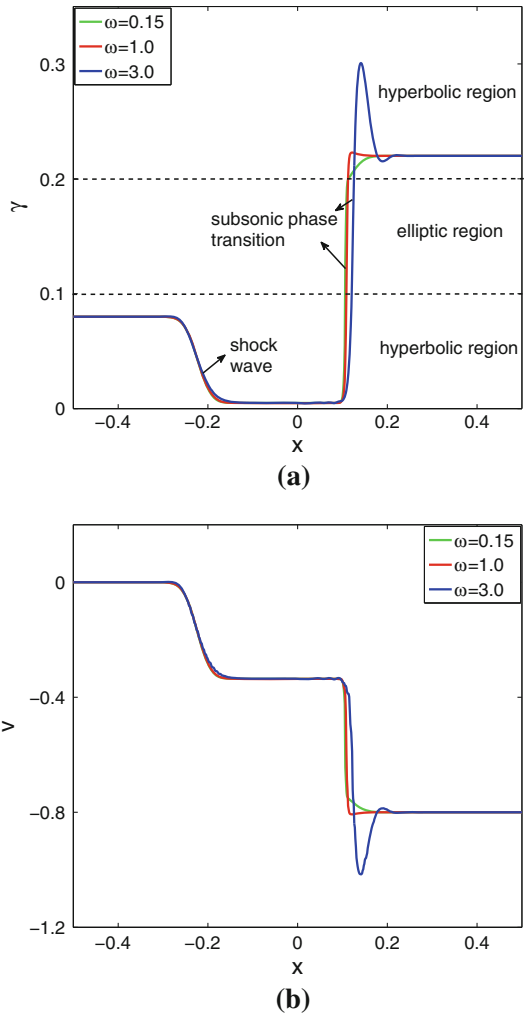

Fig. 6 Phase transitions in an elastic solid model with trilinear stress–strain relation σ, initial condition B, various ω, $M = 800$. **a** Strain γ. **b** Velocity v

6 Numerical Experiments

In this section, we describe three numerical experiments to investigate the performance of the proposed LDG scheme. Examples 6.1 and 6.2 are model test cases for phase transition in an elastic solid. Numerical simulations for compressible fluids with a liquid and vapor phase and the Van der Waals equation of state are shown in Example 6.3. For the first test case, which has a trilinear σ function, we computed the exact solution by following the analysis in [2], with the kinetic relation specified in [1]. This model problem was also studied by Cockburn and Gau [13] using a finite difference method, but their calculations only showed convergence to the exact solution for certain values of the coefficients in the VC-equations. In all computations, we employ the LDG scheme (2.5), (2.7) with numerical fluxes given by (2.6) and (2.8).

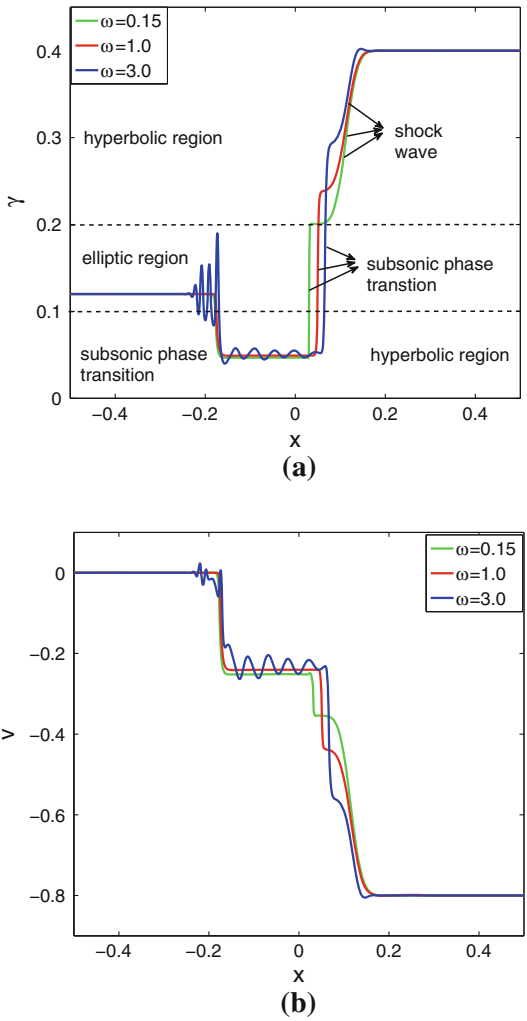

Fig. 7 Phase transitions in an elastic solid model with trilinear stress–strain relation σ, initial condition C, various ω, $M = 800$. **a** Strain γ. **b** Velocity v

Example 6.1 Piecewise linear stress–strain curve

For the trilinear stress–strain relation (5.3), we use the following parameters:

$$\gamma_M = 0.1,\ \gamma_m = 0.2,\ \mu_1 = 20,\ \mu_2 = 10,\ \mu_3 = 5,\ b = 3.$$

These conditions were also studied in [13]. The parameters ν, λ are chosen as (5.1) and (5.2), and the initial conditions are given by:

$$A: \quad \gamma(x,0) = \begin{cases} 0.3, & x < 0, \\ 0.4, & x > 0, \end{cases} \qquad v(x,0) = \begin{cases} 0, & x < 0, \\ -0.8, & x > 0, \end{cases} \tag{6.1}$$

which is the most challenging Riemann problem among all possible types of solutions, and includes two phase transitions and two shocks.

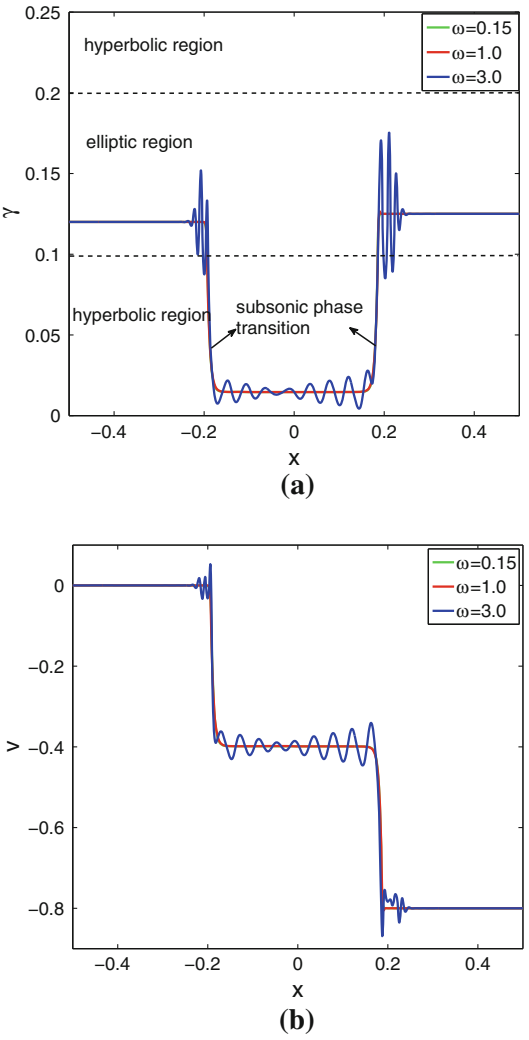

Fig. 8 Phase transitions in an elastic solid model with trilinear stress–strain relation σ, initial condition D, various ω, $M = 800$. The solutions of $\omega = 0.15$ and $\omega = 1.0$ are almost the same. **a** Strain γ. **b** Velocity v

The computational domain $[-0.5,\ 0.5]$ is discretized uniformly by M elements, and we impose the following boundary conditions:

$$\begin{cases} \gamma_0^L = \gamma_0^R, \quad \gamma_M^R = \gamma_M^L, \\ v_0^L = v_0^R, \quad v_M^R = v_M^L. \end{cases}$$

We tested the LDG scheme for the solution of the VC-equations (2.1) with piecewise constant, linear and quadratic polynomial basis functions, and compared the results at time $T_{end} = 0.05$ with the exact solution. Here, we only present the results for quadratic polynomials.

First, we compare the exact solution and the numerical solutions in Fig. 4 for piecewise quadratic basis functions and $\omega = 1.0$ using various mesh resolutions. From this figure, it is clear that the numerical solutions converge well to the exact solution. As expected, there are shock waves and phase transitions in γ: for example, the left value of γ jumps from the

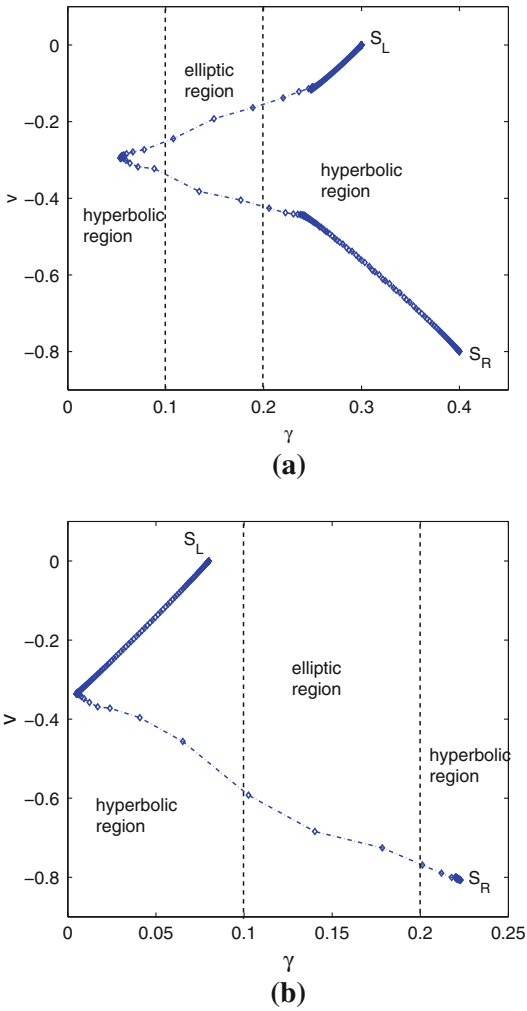

Fig. 9 Phase transitions in an elastic solid model with trilinear stress–strain relation σ, trace of the numerical solution, $\omega = 1.0$. **a** Initial condition A. **b** Initial condition B

hyperbolic state 0.3 (phase 3) to 0.25 (also in phase 3) with a shock wave, then goes through the elliptic region to 0.05 (phase 1), which gives a phase transition. Next, γ changes phase from phase 1 to phase 3, followed by a shock to the right initial γ state.

Note also that the solution at the phase boundaries remains monotonic without the use of a limiter. Figure 5 describes the numerical results of the LDG scheme with quadratic polynomial basis functions for $\omega = 0.15$, 1.0 and 3.0, when initially both γ values are outside the elliptic region. The effect of changing ω on the solution near the phase boundary is rather small, but relatively large near the shock waves in the hyperbolic region. As can be seen by comparison with Fig. 5, values $\omega \leq 1$ give better agreement with the exact solution.

If we compare our LDG results with the results of the finite difference method discussed in [13], then the LDG scheme shows the following improvements:

– for $\omega = 0.15$ and a fixed mesh resolution e.g. $M = 800$, the solutions of the LDG scheme in Fig. 5 are more accurate than those obtained with the finite difference method presented in [13];

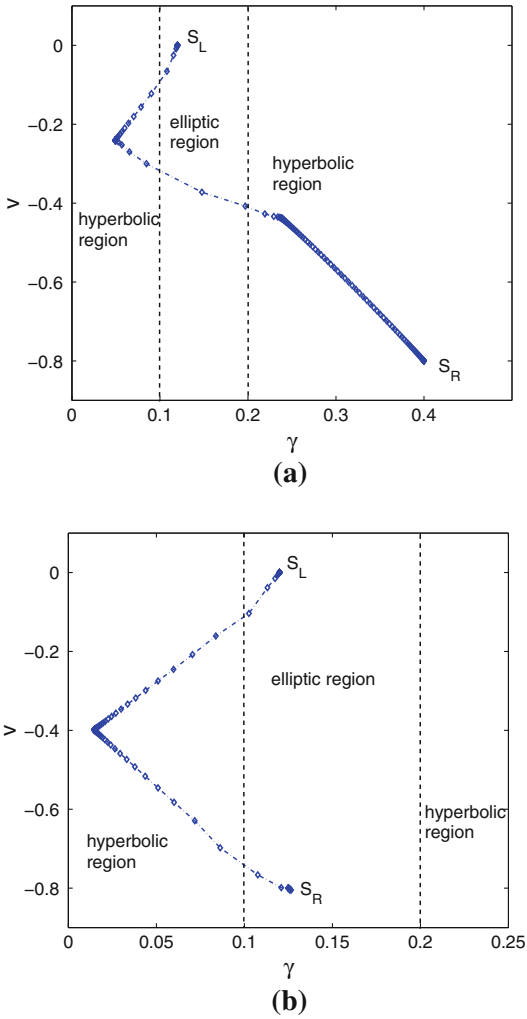

Fig. 10 Phase transitions in an elastic solid model with trilinear stress–strain relation σ, trace of the numerical solution, $\omega = 1.0$. **a** Initial condition C. **b** Initial condition D

– for the parameter $\beta = 1.0$, the numerical solutions of the finite difference method [13] converge to a wrong solution, while the LDG results converge to the exact solution.

Apart from the initial condition (6.1), we also explore three other sets of initial conditions depending on whether the initial value of γ is in the elliptic or hyperbolic region.

B: Both initial $\gamma-$values are in the hyperbolic region, but close to the elliptic region,

$$\gamma(x,0) = \begin{cases} 0.08, & x < 0, \\ 0.22, & x > 0. \end{cases} \tag{6.2}$$

C: One initial $\gamma-$value is inside the elliptic region,

$$\gamma(x,0) = \begin{cases} 0.12, & x < 0, \\ 0.40, & x > 0. \end{cases} \tag{6.3}$$

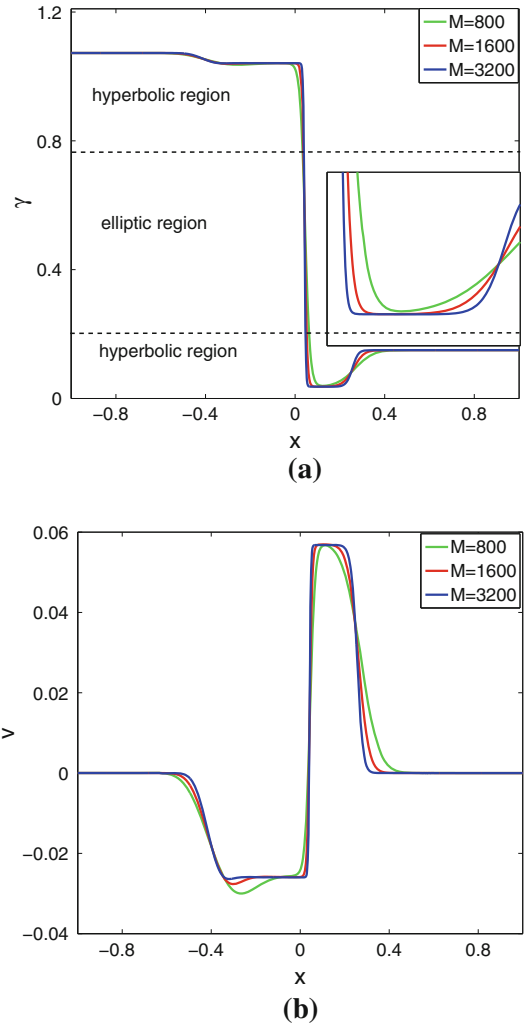

Fig. 11 Phase transition in an elastic solid model with cubic stress–strain relation σ, $\omega = 1.0$. **a** Strain γ. **b** Velocity v

D: Both initial $\gamma-$values are inside the elliptic region,

$$\gamma(x,0) = \begin{cases} 0.120, & x < 0, \\ 0.125, & x > 0. \end{cases} \tag{6.4}$$

We use the same initial condition (6.1) for the velocity in all these test cases.

The results of the LDG calculations of γ, v for the initial conditions B, C, D are shown in Figs. 6, 7, 8. From these results, we observe that the solutions oscillate and dissipate most near the phase boundary when $\omega = 3.0$. We also plot the traces of the numerical solution (points connecting initial $\gamma-$values S_L and S_R) for various initial conditions in Figs. 9 and 10. One important observation is that the solutions never stay inside the elliptic region:

– when an initial state is outside the elliptic region, or the solution evolves to the boundary of the hyperbolic region, the solution will immediately go through the elliptic region to another hyperbolic region;

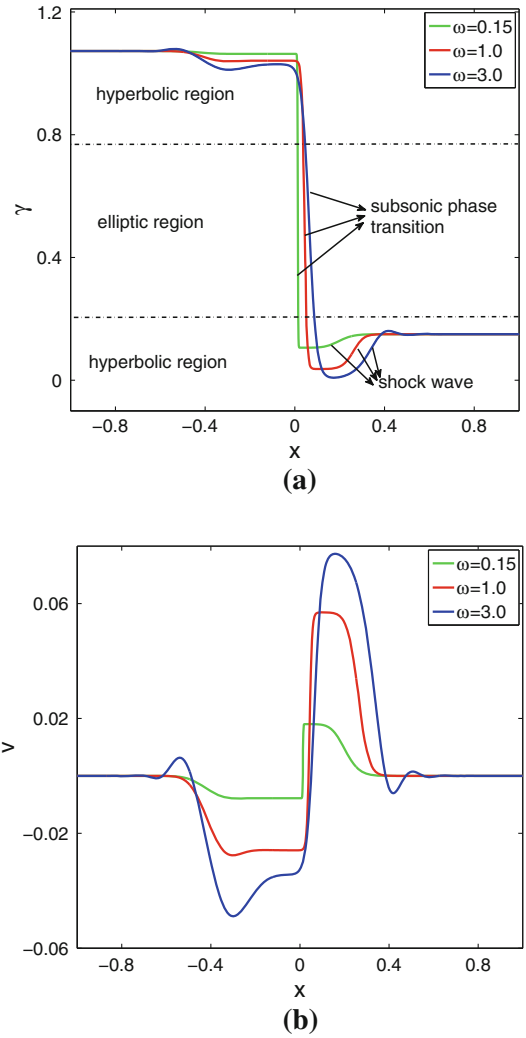

Fig. 12 Phase transition in an elastic solid model with cubic stress–strain relation σ, $M = 1{,}600$. **a** Strain γ. **b** Velocity v

– when the initial state is inside the elliptic region, the solution will move quickly to a hyperbolic region.

Example 6.2 Cubic stress–strain curve

In this section, we present results of the LDG scheme for the VC-equations (2.1) with a cubic stress–strain relation

$$\sigma(\gamma) = \gamma(\gamma - 0.5)(\gamma - 1), \tag{6.5}$$

see Fig. 2.

The initial data are given as:

$$\gamma_0(x) = \begin{cases} 1.07265, & x < 0, \\ 0.15000, & x > 0, \end{cases} \quad v_0(x) \equiv 0. \tag{6.6}$$

Table 1 Accuracy test for modified VC-equations (6.8) with the exact solution (6.7). Periodic boundary condition. Uniform meshes with M cells at time $t = 0.2$

	M	$L^\infty-$ error	order	L^2- error	order
P^0	20	7.33E-02	–	5.54E-02	–
	40	3.54E-02	1.05	2.67E-02	1.05
	80	1.73E-02	1.03	1.32E-02	1.02
	160	8.58E-03	1.01	6.55E-03	1.01
	320	4.28E-03	1.00	3.27E-03	1.00
P^1	20	8.11E-03	–	5.80E-03	–
	40	2.05E-03	1.98	1.45E-03	2.00
	80	5.14E-04	2.00	3.63E-04	2.00
	160	1.28E-04	2.00	9.09E-05	2.00
	320	3.21E-05	2.00	2.27E-05	2.00
P^2	20	2.57E-04	–	1.91E-04	–
	40	3.22E-05	2.99	2.34E-05	3.03
	80	4.04E-06	3.00	2.89E-06	3.02
	160	5.05E-07	3.00	3.59E-07	3.01
	320	6.31E-08	3.00	4.47E-08	3.00

From the numerical results in Figs. 11 and 12, it is easy to see that:

1. the numerical results in Figs. 11 and 12 are very similar to those of the trilinear stress–strain relation (Figs. 4, 5, 6, 7, 8, 9, 10): both of these two test cases include shocks and phase transitions;
2. Figure 12 shows the results for quadratic polynomials using various ω values for a fixed mesh resolution $M = 1,600$, which indicates that solutions with larger values of ω have more dissipation at the phase boundary;
3. comparing the LDG results with those of the finite difference method in [13], the LDG results are much closer to the exact solution. For example, we don't observe numerical oscillations around the first phase transition in the LDG scheme (see Figs. 11 and 12), which exist in the velocity figures computed with the finite difference method [13].

In order to verify the a priori error analysis discussed in Sect. 4, we also selected the following smooth exact solution,

$$\gamma(x,t) = 0.6 + 0.5\sin(2\pi x + t), \quad v(x,t) = 0.1\cos(2\pi x - t), \tag{6.7}$$

which satisfies the VC system (2.1) with source terms $a(x,t),\ b(x,t)$.

$$\begin{cases} \gamma_t = v_x + a(x,t), \\ v_t = \sigma(\gamma)_x + \nu v_{xx} - \lambda\gamma_{xxx} + b(x,t). \end{cases} \tag{6.8}$$

We compute the error of γ in the L^∞ and L^2 norm, and obtain the order of accuracy. The results are presented in Table 1, which shows that for k-th order polynomials the LDG discretization has $k+1$-th order accuracy. We emphasize that the numerical results are better than the theoretical error estimate given in Sect. 4.

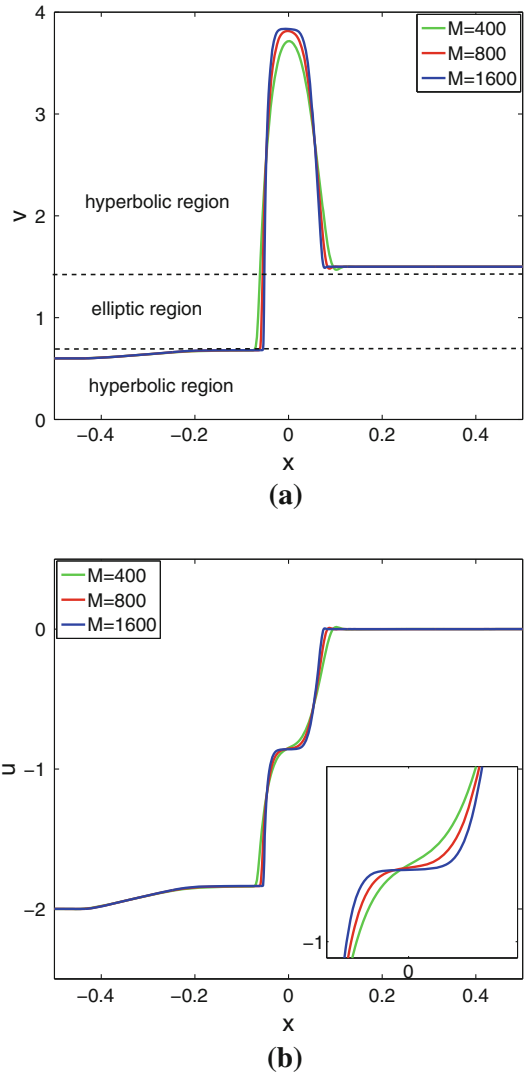

Fig. 13 Van der Waals fluid, initial condition E, $\omega = 1.0$, $T_{end} = 0.15$. **a** Specific volume. **b** Velocity

Example 6.3 General non-monotonic stress–strain curve

Next, we investigate the LDG scheme for (2.1) with a general non-monotonic stress–strain relation. In this part, we consider a VC model for a compressible fluid with a liquid and vapor phase [9], given by

$$\begin{cases} v_t - u_x = 0, \\ u_t + P(v)_x = \nu u_{xx} - \lambda v_{xxx}, \end{cases} \tag{6.9}$$

where $v = 1/\rho$ is the specific volume, u the particle velocity. The Van der Waals equation of state is given by:

$$P(v, T) = \frac{RT}{v - b} - \frac{a}{v^2},$$

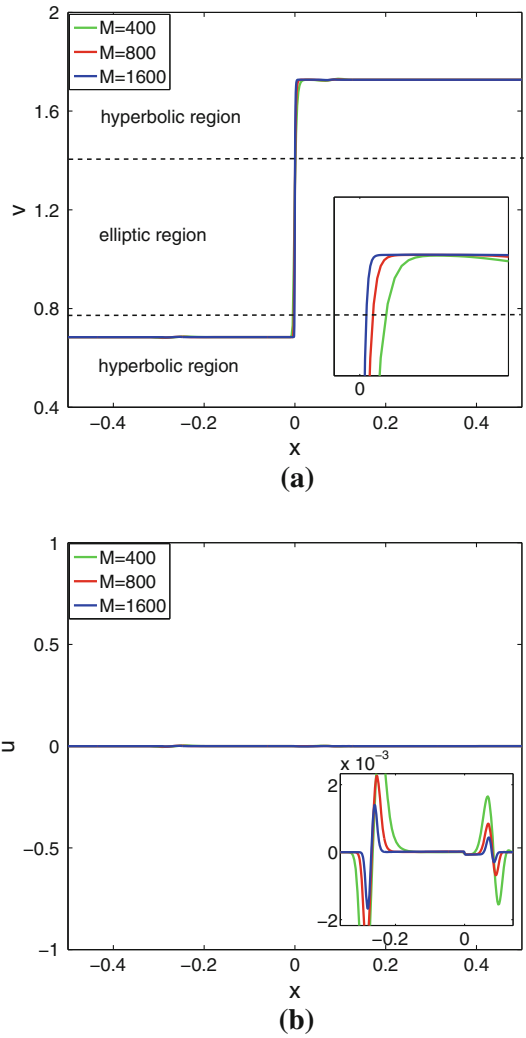

Fig. 14 Van der Waals fluid, initial condition F, $\omega = 1.0,\ T_{end} = 0.2$. **a** Specific volume. **b** Velocity

where $a,\ b,\ R$ are constants with the temperature $T > 0$ fixed. We use the non-dimensional formulation in which:

$$a = 3,\ b = \frac{1}{3},\ R = \frac{8}{3},$$

and take the relative temperature to be $T = 0.95$ (See Fig. 3).

The system (6.9) under consideration is close to that for (1.2) except for the difference between $\sigma(\gamma)$ and $-P(v)$, which are both increasing-decreasing-increasing functions. With appropriate viscosity and capillarity coefficients, for example $\nu = h,\ \lambda = \omega\nu^2$ with $\omega = 0.5,\ 1.0$ and 3.0, we can obtain the same results as those obtained in [9]. Two test cases are considered, both of them use meshes with 400, 800 and 1,600 elements.

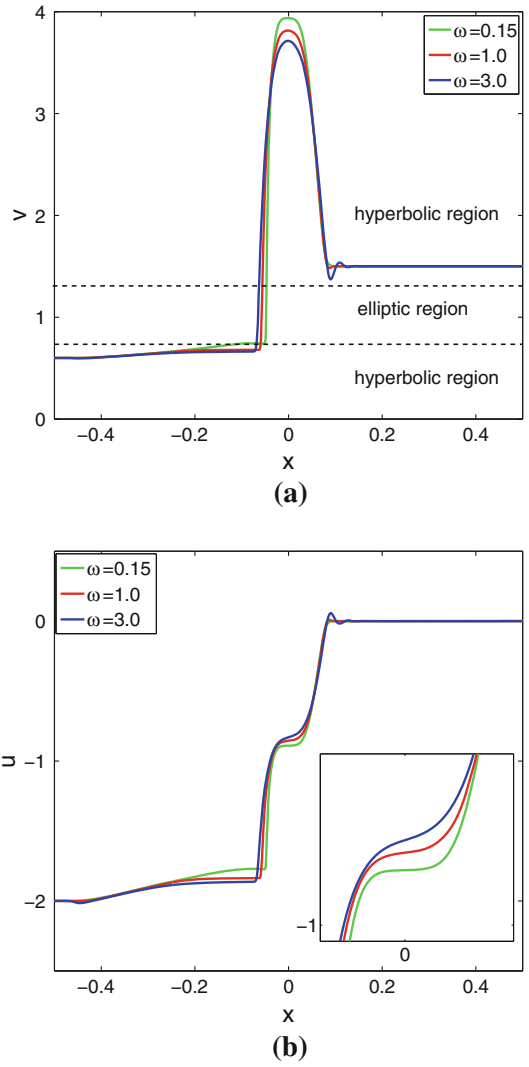

Fig. 15 Van der Waals fluid, initial condition E, $M = 800$, $T_{end} = 0.15$. **a** Specific volume. **b** Velocity

E: Propagating phase boundary with initial conditions:

$$v(x,0) = \begin{cases} 0.6, & x < 0, \\ 1.5, & x > 0, \end{cases} \qquad u(x,0) = \begin{cases} -2.0, & x < 0, \\ 0.0, & x > 0. \end{cases}$$

The solutions of the LDG method are considered at time $T_{end} = 0.15$.

F: Stationary phase boundary with initial conditions:

$$v(x,0) = \begin{cases} 0.684117091, & x < 0, \\ 1.72700257, & x > 0, \end{cases} \qquad u(x,0) \equiv 0. \tag{6.10}$$

This initial condition is very close to the Maxwell stationary phase boundary and the LDG method should keep the Maxwell discontinuity stationary. The numerical results are shown at $T_{end} = 0.2$.

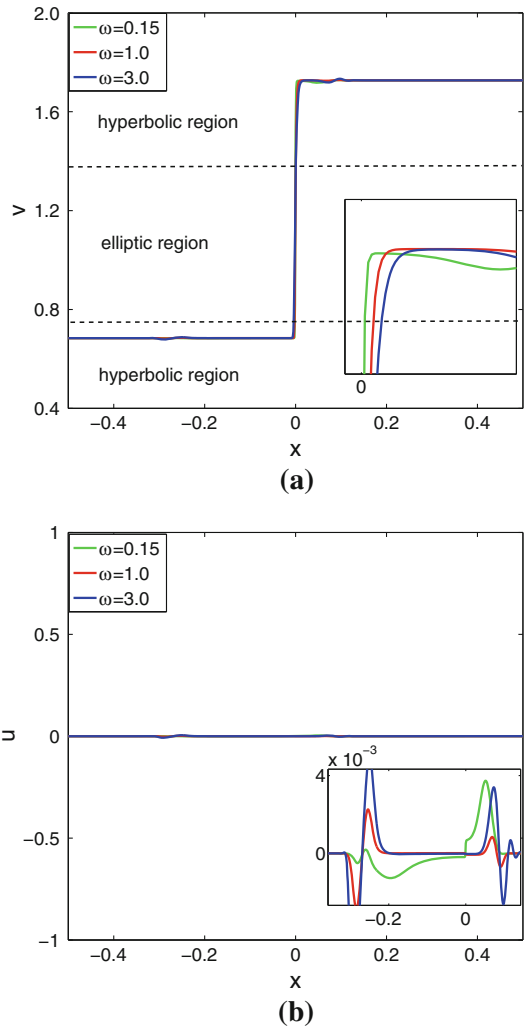

Fig. 16 Van der Waals fluid, initial condition F, $M = 800$, $T_{end} = 0.2$. **a** Specific volume. **b** Velocity

Figures 13 and 14 show solutions obtained with the LDG method for various mesh resolutions $M = 400,\ 800, 1{,}600$; Figs. 15 and 16 show solutions with various values of ω. From these figures, we can draw several conclusions:

1. The numerical solutions converge consistently;
2. Figures 13 and 15 show that the propagating phase boundary case also includes both shock waves and phase transitions;
3. Figures 14 and 16 show that the LDG method keeps the Maxwell discontinuity stationary;
4. Figure 15 shows for various values of ω that the width of the jump in the specific volume v is larger for bigger ω.

From this test case, we conclude that the LDG method that we presented in this paper also applies to the VC system (2.1) with general nonlinear stress–strain relations σ.

7 Conclusion

In this article, we have designed, analyzed and tested an LDG method for the numerical solution of the VC equations modeling the propagation of phase transitions in solids [13] and fluids [9]. L^2-stability is proved for general solutions of the VC system. We also provide an a priori error estimate of the semi-discrete LDG method when the solutions are assumed to be sufficiently smooth and the stress–strain relation in (1.1) and (2.1) is linear. Also, a linear stability analysis is performed to obtain an estimate for a stable time step in the Runge–Kutta time integration method. Numerical experiments show that the results of the LDG scheme converge well to the exact solution of the phase transition model given by (1.1). Moreover, the LDG scheme can also be applied to a model of Van der Waals fluids [9] when the artificial viscosity is taken to be proportional to Δx. The error analysis for a linear stress–strain relation shows that the LDG discretization of the phase transition model (1.1) is of optimal order, when $\lambda \sim Ch$ and $\lambda, \nu \downarrow 0$, with $\omega = 2\sqrt{\lambda}/\nu$ fixed. For finite values of λ, ν, the error bound is suboptimal, but numerical results indicate that in practice still an optimal convergence rate is obtained.

In the future, we will consider the extension of the LDG scheme to the non-isothermal Navier–Stokes–Korteweg equations with a Van der Waals equation of state [21]. This will be a challenge because this non-isothermal flow model contains highly nonlinear high-order terms.

Acknowledgments L.Tian acknowledges a fellowship from the China Scholarship Council (CSC) giving the opportunity and financial support to study at the University of Twente.

References

1. Abeyaratne, R., Knowles, J.K.: Implications of viscosity and strain-gradient effects for the kinetics of propagating phase boundaries in solids. SIAM J. Appl. Math. **51**, 1205–1221 (1991)
2. Abeyaratne, R., Knowles, J.K.: Kinetic relations and the propagation of phase boundaries in solids. Arch. Ration. Mech. Anal. **114**, 119–154 (1991)
3. Abeyaratne, R., Knowles, J.K.: Evolution of Phase Transitions: A Continuum Theory. Cambridge University Press, Cambridge (2006)
4. Berezovski, A., Maugin, G.A.: Numerical simulation of phase-transition front propagation in thermoelastic solids. In: Quintela, P., Salgado, P., Bermudez de Castro, A., Gomez, D. (eds.) Numerical Mathematics and Advanced Applications (Proceedings of ENUMATH 2005), pp. 703–711. Springer, Berlin (2006)
5. Boutin, B., Chalons, C., Lagoutiere, F., LeFloch, P.G.: Convergent and conservative schemes for nonclassical solutions based on kinetic relations. Interfaces Free Boundaries **10**, 399–421 (2008)
6. Chalons, C.: Transport-equilibrium schemes for computing nonclassical shocks. Comptes Rendus Mathematique **342**, 623–626 (2006)
7. Chalons, C., Coulombel, J.F.: Relaxation approximation of the Euler equations. J. Math. Anal. Appl. **348**, 872–893 (2008)
8. Chalons, C., Goatin, P.: Godunov scheme and sampling technique for computing phase transitions in traffic flow modeling. Interfaces Free Boundaries **10**, 197–221 (2008)
9. Chalons, C., LeFloch, P.G.: High-order entropy-conservative schemes and kinetic relations for van der Waals fluids. J. Comput. Phys. **168**, 184–206 (2001)
10. Chalons, C., LeFloch, P.G.: Computing under-compressive waves with the random choice scheme. Nonclassical shock waves. Interfaces Free Boundaries **5**, 129–158 (2003)
11. Chalons, C., Coquel, F., Engel, P., Rohde, C.: Fast relaxation solvers for hyperbolic-elliptic phase transition problems. SIAM J. Sci. Comput. **34**, 1753–1776 (2012)
12. Ciarlet, P.G.: The Finite Element Method for Elliptic Problems. North Holland, Amsterdam (1978)
13. Cockburn, B., Gau, H.: A model numerical scheme for the propagation of phase transitions in solids. SIAM J. Sci. Comput. **17**, 1092–1121 (1996)

14. Cockburn, B., Shu, C.W.: The local discontinuous Galerkin method for time-dependent convection-diffusion systems. SIAM J. Numer. Anal. **141**, 2440–2463 (1998)
15. Colombo, R.M., Corli, A.: Sonic and kinetic phase transitions with applications to Chapman–Jouguet deflagrations. Math. Methods Appl. Sci. **27**, 843–864 (2004)
16. Coquel, F., Perthame, B.: Relaxation of energy and approximate Riemann solvers for general pressure laws in fluid dynamics. SIAM J. Numer. Anal. **35**, 2223–2249 (1998)
17. Haink, J., Rohde, C.: Local discontinuous Galerkin schemes for model problems in phase transition theory. Commun. Comput. Phys. **4**, 860–893 (2008)
18. LeFloch, P.: Propagating phase boundaries: formulation of the problem and existence via the Glimm method. Arch. Ration. Mech. Anal. **123**, 153–197 (1993)
19. LeFloch, P.G.: Hyperbolic Systems of Conservation Laws: The Theory of Classical and Nonclassical Shock Waves, vol. 35. Birkhäuser, Basel (2002)
20. Merkle, C., Rohde, C.: The sharp-interface approach for fluids with phase change: Riemann problems and ghost fluid techniques. Math. Model. Numer. Anal. **41**, 1089–1123 (2007)
21. Pecenko, A., Van Deurzen, L.G.M., Kuerten, J.G.M., Van der Geld, C.W.M.: Non-isothermal two-phase flow with a diffuse-interface model. Int. J. Multiph. Flow **37**, 149–165 (2011)
22. Shu, C.W., Osher, S.: Efficient implementation of essentially non-oscillatory shock-capturing schemes. J. Comput. Phys. **77**, 439–471 (1988)
23. Slemrod, M.: Dynamic phase transitions in a van der Waals fluid. J. Differ. Equ. **52**, 1–23 (1984)
24. Truskinovsky, L.: Kinks versus shocks, Shock induced transitions and phase structures in general media. IMA Vol. Math. Appl. **52**, 185–229 (1993)
25. Xu, Y., Shu, C.W.: A local discontinuous Galerkin method for the Camassa–Holm equation. SIAM J. Numer. Anal. **46**, 1998–2021 (2008)
26. Xu, Y., Shu, C.W.: Local discontinuous Galerkin methods for high-order time-dependent partial differential equations. Commun. Comput. Phys. **7**, 1–46 (2010)
27. Xu, Y., Shu, C.W.: Optimal error estimates of the semi-discrete local discontinuous Galerkin methods for high order wave equations. SIAM J. Numer. Anal. **50**, 79–104 (2012)
28. Yan, J., Shu, C.W.: A local discontinuous Galerkin method for KdV type equations. SIAM J. Numer. Anal. **40**, 769–791 (2002)
29. Zhong, X.G., Hou, T.Y., LeFloch, P.G.: Computational methods for propagating phase boundaries. J. Comput. Phys. **124**, 192–216 (1996)